

## Design of an Orthomode Transducer in Gap Waveguide Technology

*Master of Science Thesis in the program Communication Engineering*

ALI IMRAN SANDHU

Antenn Group, Department of Signals & Systems  
Chalmers University of Technology  
Göteborg, Sweden, September 2010



The Author grants to Chalmers University of Technology the non-exclusive right to publish the Work electronically and in a non-commercial purpose make it accessible on the Internet. The Author warrants that he/she is the author to the Work, and warrants that the Work does not contain text, pictures or other material that violates copyright law.

The Author shall, when transferring the rights of the Work to a third party (for example a publisher or a company), acknowledge the third party about this agreement. If the Author has signed a copyright agreement with a third party regarding the Work, the Author warrants hereby that he/she has obtained any necessary permission from this third party to let Chalmers University of Technology store the Work electronically and make it accessible on the Internet.

Design of an Orthomode Transducer in Gap Waveguide Technology  
ALI IMRAN SANDHU

© ALI IMRAN SANDHU, 2010

Examiner: Prof. Per-Simon Kildal

Technical report no 2010:xx  
Antenna Group, Department of Signals & Systems  
Chalmers University of Technology  
SE-41296 Gteborg  
Sweden  
Telephone +46 (0) 31-772 1000

Cover: Picture shows the 3D OMT structure with magnitude E field inside, simulated in HFSS

Antenna Group, Department of Signals & Systems  
Gteborg, Sweden September 2010

*I would like to dedicate my work to my family. I believe that I have made it possible merely due to the prayers and great moral support from my parents throughout my studies. Special dedications to my daughter and my wife for their patience and support being away from me.*

# Acknowledgements

I owe my deepest gratitude to all of those who made this thesis possible. I would like to thank

- Professor Per-Simon Kildal for his confidence in me that I could complete this master project and his excellent supervision. He provided tremendous support, guidance, and motivation throughout this project. Thanks for always having time to answer questions and replying to emails almost instantaneously. It has been a rewarding and unique experience to work and study under your supervision!
- Professor Ahmed A.Kishk for being so nice and devoted towards my thesis progress. I have always found him clearing my concepts, even during weekends and late at evenings. I must appreciate his 3D drawing capabilities, which helped me a lot to visualise and implement the designs. I am very thankful for his sincere guidance regarding my thesis work and future studies.
- Dr. Jian Yang, without whom's support this thesis would not have been possible. I have always felt comfortable in bothering him for discussions related to my thesis work and future studies as well. I would like to appreciate his sincere guidance related to the antenna course. He was not related to my master thesis, even then he always assisted me on issues related to HFSS simulations and theoretical concepts. I cannot limit my gratitude for him in words.
- Anders Edquist from Ansoft support. He has always assisted me in resolving complex as well as very basic issues related to my simulations. He always replied my emails frequently with detailed images and technical notes which helped me in learning the software to a greater extent.
- Ashraf for his support. Elenna has been a very nice office mate. She has assisted me in clarifying many concepts. I will remember her laughs.
- The fellow students and the faculty members who made MPCOM program an interesting yet an enjoyable course. A very special thanks to the Chalmers admission council, who gave me an opportunity to pursue my master studies, and for providing me more than enough resources to utilize. I will treasure the friendships and memories that I have taken from here.

# Abstract

Ortho-mode transducer (OMT) is a waveguide structure capable of discriminating two independent signals of the orthogonal dominant modes provided at the common equipment port and supplying them to the fundamental mode of the allocated single signal interface ports, maintaining a good match at all electrical ports and high cross-polarization discrimination between the independent signals.

Gap waveguide is a new waveguide technology recently introduced in [1] and experimentally verified in [2]. It is formed inside the gap between the two metallic surfaces one of which is provided with a texture or thin multilayer structure that is used to realize conducting ridges surrounded by a high impedance surface of some kind, which might ideally be a PMC surface. Gap waveguides have made use of bed of nails [3], as a high impedance surface for parallel plate mode suppression, which has resulted in a band stop for more than an octave bandwidth(2:1). Since wave propagation is made prohibited in any arbitrary direction other than the conducting ridge, mechanical joints can be applied far away from the propagation path. This gives very good electrical performance, since it prevents leakage of electromagnetic energy even at high frequencies such as for millimeter and sub millimeter waves, when waveguides are manufactured in two pieces. Gap waveguides are planner and much cheaper to manufacture as compared to hollow waveguides, furthermore they have been very promising, being very wide band and low loss than alternative so called substrate integrated waveguides(SIW).

Arkivator telecom has shown interest in the gap waveguide technology, therefore in collaboration with Chalmers, Arkivator telecom has provided an opportunity to investigate whether if the design of passive microwave devices in gap waveguide technology is practically realizable, along with a good overall electrical performance. An OMT in gap waveguide technology has been designed, optimized, and simulated for approximately 7 percent bandwidth centered at 42 GHz. The simulations have been done using HFSS. The device exhibits a return loss better than 28dB and isolation better than 35dB for the desired frequency band. The device has shown excellent circular polarization performance even better than the existing standard waveguide based alternatives. The axial ratio was found to be below 0.2dB with a cross polar isolation better than 40dB.

# Preface

This thesis is submitted in partial fulfilment of the requirements for a Master's Degree in communication engineering at Chalmers University of Technology. It contains work done from January to August 2010. My supervisors on this project were Prof. Per-Simon Kildal, Chalmers University of Technology and Prof. Ahmed A. Kishk, University of Mississippi. This thesis has been made solely by the author; most of the text however, is based on the research of Prof. Per-Simon and his research group, and I have done my best to provide references for these sources.

This thesis is based on designing, simulating and measuring an orthomode transducer (OMT) in the recently introduced gap waveguide technology, which has proved to be very wide band and less lossy. The major advantage of the ridge gap waveguide as compared to hollow waveguides is that they are simpler and much cheaper to manufacture, in particular at high frequencies such as for millimetre and sub millimetre waves. The latter is due to the fact that there are no mechanical joints required, across which electric currents must flow. Arkivator Telecom has shown interest in the newly introduced gap waveguide technology; therefore in collaboration with Chalmers, Arkivator Telecom has provided an opportunity to investigate whether if the design of passive microwave devices in gap waveguide technology is practically realizable, along with a good overall electrical performance. This OMT design is among several other projects in pipeline, funded and industrially supported by Arkivator Telecom.

This dissertation presents the essential theoretical context along with a few physically realizable alternatives based on extensive simulations to design the OMT in the gap waveguide technology. Furthermore the report is structured, so that every chapter is dedicated to an individual component associated with the OMT. The Introduction (Chapter 1) presents information on the device's electrical performance requirements along with a brief description of various frequently used technical terminologies. Chapter 2 (Orthomode Transducer) covers fundamental concepts to understand the working principle of an OMT.

Chapter 3 (Gap Waveguide) describes the principle, operation and detailed analysis of gap waveguides along with a brief introduction to PMC realization approaches. Most of the context of this chapter is taken from the research of Prof. Per Simon Kildal and his

fellow researchers. Chapter 4 and Chapter 5 describes a brief theoretical content related to septum polarizers and quarter wave plates respectively.

Chapter 6 is dedicated to the design and simulations for individual components associated with the OMT. In addition to the simulations, a comparative discussion for a few alternatives in terms of performance and fabrication limitations has been included also. Chapter 7 presents the re-optimized designs that incorporate all necessary fabrication tolerances. These designs have been placed forward for fabrication. The results presented in this chapter are expected to produce a very close agreement with the prototype's measurements. This last chapter is followed by Conclusion, summarizing the so far progress and future work, followed by the Appendix that has a few useful MATLAB programs.

# Contents

<b>Acknowledgements</b>	<b>iii</b>
<b>Abstract</b>	<b>iv</b>
<b>Preface</b>	<b>v</b>
<b>List of Figures</b>	<b>ix</b>
<b>Abbreviations</b>	<b>xi</b>
<b>1 Introduction</b>	<b>1</b>
1.1 Design Requirements . . . . .	2
1.2 Basic Theory . . . . .	2
1.2.1 Plane Waves and their Polarization . . . . .	2
1.2.1.1 Linear Polarization . . . . .	3
1.2.1.2 Circular Polarization . . . . .	3
1.2.2 Axial Ratio . . . . .	4
1.2.3 Cross Polar Isolation . . . . .	4
1.2.4 Return Loss . . . . .	4
1.2.5 Isolation . . . . .	4
<b>2 Orthomode Transduce (OMT)</b>	<b>6</b>
<b>3 Gap Waveguide</b>	<b>9</b>
3.1 Introduction . . . . .	9
3.2 High Impedance Surfaces . . . . .	10
3.2.1 PMC Realization Using Bed of Nails . . . . .	11
3.3 Ridge Gap Waveguide . . . . .	12
3.3.1 Physical Theory . . . . .	13
3.3.2 Principle of Operation . . . . .	13
3.3.3 Similarities With Other Transmission Lines & Waveguides . . . . .	15
3.3.4 Designing For Desired Characteristic Impedance . . . . .	16
3.4 Analysis . . . . .	16
<b>4 Septum Polarizer</b>	<b>18</b>
4.1 Introduction . . . . .	18
4.2 Operation . . . . .	18
4.2.1 Even-Mode Excitation . . . . .	19

4.2.2	Odd-Mode Excitation . . . . .	20
4.3	Mathematical formulation . . . . .	21
<b>5</b>	<b>Quarter Wave Plate</b>	<b>23</b>
5.1	Introduction . . . . .	23
5.2	Operation . . . . .	23
<b>6</b>	<b>Design &amp; Simulation Analysis</b>	<b>26</b>
6.1	CST vs HFSS Performance Analysis . . . . .	26
6.2	Ridge Gap Waveguide . . . . .	28
6.3	Septum Polarizer . . . . .	29
6.3.1	Standard Waveguide Technology . . . . .	29
6.3.2	Gap Waveguide Technology . . . . .	32
6.3.2.1	Single Layer Pin Texture . . . . .	33
6.3.2.2	Double Layer Pin Texture . . . . .	36
6.4	Quarter Wave Plate . . . . .	40
6.5	Right Angle E Bend . . . . .	41
6.6	Quadratic to Circular Transition . . . . .	42
<b>7</b>	<b>Prototype Design</b>	<b>44</b>
7.1	Simulated Results . . . . .	45
7.2	Prototype CAD Analysis . . . . .	46
7.3	Downscaled Structure Analysis . . . . .	48
7.3.1	Input E bend optimization . . . . .	48
7.3.2	Quadratic to Circular Transition optimization . . . . .	48
7.4	Optimized Double Layer Pin Structure . . . . .	51
7.5	Optimized Single Layer Pin Prototype Model . . . . .	53
	<b>Bibliography</b>	<b>56</b>
	<b>Conclusion</b>	<b>56</b>
	<b>MATLAB Code</b>	<b>59</b>

# List of Figures

2.1	Principle equivalent circuit of an OMT. . . . .	7
3.1	Transversely corrugated soft surface . . . . .	10
3.2	Manufactured metal lid with pins (left), 2-D color plots of vert. E field distribution(right) inside the gap between the microstrip board and the lid of the metal box, both (a) with smooth metal lid and (b) with a lid of nails. . . . .	12
3.3	Cross-sectional views of ideal gap waveguide and its similarities with other transmission lines . . . . .	13
3.4	Dispersion diagram for the gap waveguide . . . . .	15
4.1	Common type of septum polarizers. . . . .	19
4.2	Propagation of parallel component (top) followed by propagation of normal component (middle) and total E field (bottom). . . . .	20
4.3	Polarization operation. . . . .	21
5.1	Incident wave decomposition inside a square waveguide. . . . .	24
6.1	Standard waveguide based OMT, fabricated with aluminium, operating at (50 - 56) GHz band . . . . .	27
6.2	Return Loss and Insertion Loss Simulation Comparison . . . . .	27
6.3	Ridge Gap Waveguide Geometry . . . . .	28
6.4	Return loss is below -30 dB for approximately 12 percent bandwidth . . . . .	29
6.5	Septum polarizer in standard waveguide technology . . . . .	30
6.6	Return Loss and Isolation Performance . . . . .	31
6.7	Axial ratio and cross polar isolation for SWG septum polarizer . . . . .	31
6.8	Return loss performance comparison for full and half pin period for GGWG . . . . .	33
6.9	Return loss and circular polarization performance analysis for full plate GWGSP . . . . .	34
6.10	Full plate and half plate(truncated) septum geometry . . . . .	35
6.11	Return loss for septum polarizer with half plate . . . . .	35
6.12	Circular polarization and isolation comparison . . . . .	36
6.13	Front view of double layer pin texture based septum polarizer. Red bounded region defines the septum plate geometry . . . . .	37
6.14	Return loss performance of various double pin textured models . . . . .	38
6.15	Front view of double layer pin texture based septum polarizer. Red bounded region defines the septum plate geometry . . . . .	39
6.16	3D view of the quarter wave plate . . . . .	40
6.17	Return loss performance for the quarter wave plate . . . . .	41

6.18	Geometrical view of the right angle E bend . . . . .	41
6.19	Return loss performance for the right angle E bend . . . . .	42
6.20	Geometrical view of the quadratic to circular transition . . . . .	42
6.21	Return loss performance for the quadratic to circular transition . . . . .	43
7.1	GWGSP Prototype Geometry . . . . .	44
7.2	Return loss and circular polarization performance analysis for full plate GWGSP . . . . .	45
7.3	CAD based modified geometry . . . . .	46
7.4	Return loss and isolation performance for CAD modified and re-optimized structures . . . . .	47
7.5	Axial ratio performance analysis for proposed, modified and re-optimized structures . . . . .	48
7.6	3D view and return loss performance of downscaled E bend . . . . .	49
7.7	3D view and return loss performance of downscaled QST . . . . .	50
7.8	Cross sectional view of the double layer pin structure . . . . .	51
7.9	Electrical performance for double layer pin texture . . . . .	52
7.10	3D view and return loss performance of downscaled prototype model . . .	53
7.11	Isolation and circular polarization performance . . . . .	54

# Abbreviations

<b>GWG</b>	<b>Gap Waveguide</b>
<b>GGWG</b>	<b>Groove Gap Waveguide</b>
<b>GWGSP</b>	<b>Gap Waveguide Septum Polarizer</b>
<b>RGWG</b>	<b>Ridge Gap Waveguide</b>
<b>RL</b>	<b>Return Loss</b>
<b>PMC</b>	<b>Perfect Magnetic Conductor</b>
<b>PEC</b>	<b>Perfect Electric Conductor</b>
<b>EBG</b>	<b>Electromagnetic Band Gap</b>
<b>RHC</b>	<b>Right Hand Circular</b>
<b>LHC</b>	<b>Left Hand Circular</b>
<b>TEM</b>	<b>Transverse Electro Magnetic</b>
<b>QWP</b>	<b>Quarter Wave Plate</b>

# Chapter 1

## Introduction

The objective of this master thesis was to design, simulate and measure the performance of an OMT designed in gap waveguide technology, operating for approximately 7 percent bandwidth centered at 42GHz, providing good electrical match between all the ports along with a reasonable isolation performance. Gap waveguide [1] [4] and [5] is a new type of waveguide confined in a narrow gap between two parallel metal plates, one of which is introduced to a texture or multilayer structure, which gives high surface impedance (ideally a perfect magnetic conductor) that provides suppression for the waves propagation in any arbitrary direction other than the conducting ridge. A comprehensive study to understand the gap waveguide has been presented in the following chapters.

An OMT is basically a polarization discrimination device which separates orthogonal polarizations within the same frequency band. This provide means to use two frequency channels simultaneously, thus enhances system capacity. Employing OMT's in the feed systems allows the antenna systems to operate on larger bandwidths, providing additionally enhanced capacity and versatility.

Arkivator Telecom, is a Swedish company, possesses excellence in manufacturing various antennas, reflectors and several other passive microwave devices. Major antennas that are being fabricated in Arkivator Telecom are based on the patented Hat Antenna principle, developed by Professor Per-Simon Kildal at Chalmers University of Technology in Gothenburg Sweden, which are targeted for point-to-point radio communication links. This patented design combines excellent side-lobe suppression, low cross polarization and high gain into a compact and lightweight antenna. Arkivator Telecom offers a range of such antennas between 0.2 meters and 1.2 meters with operating frequencies ranging from 10GHz to 40GHz. Arkivator Telecom has shown interest in the newly introduced gap waveguide technology; therefore in collaboration with Chalmers, Arkivator Telecom has provided an opportunity to investigate whether if the design of passive microwave devices in gap waveguide technology is practically realizable, along with a good overall

electrical performance. This OMT design is among several other projects in pipeline, funded and industrially supported by Arkivator Telecom.

## 1.1 Design Requirements

The proposed electrical specifications for this OMT are as follows:

*Frequency Band*  $\rightarrow 40.5GHz - 43.5GHz$

*Input Flange*  $\rightarrow 4.8mm \times 2.4mm$

*Circular Port Diameter*  $\rightarrow 6.186mm$

*Return Loss Performance*  $\geq 30dB$

*Isolation Performance*  $\geq 35dB$

## 1.2 Basic Theory

Before proceeding to the later chapters that will cover the complete analysis and design of various passive devices being a part of this project, it is worthy to recall some basic concepts. The terminologies described in this section have been frequently used in the following chapters. A brief description of some important terminologies are given here.

### 1.2.1 Plane Waves and their Polarization

The time harmonic E and H fields of a plane wave propagating in the positive z-direction in free space are described by [6] as

$$\mathbf{E} = E_t e^{-jkz} = [E_x \hat{x} + E_y \hat{y}] e^{-jkz} \quad (1.1)$$

$$\mathbf{H} = \frac{1}{\eta} \hat{z} \times \mathbf{E} = \frac{1}{\eta} \hat{z} \times E_t e^{-jkz} = \frac{1}{\eta} [-E_y \hat{x} + E_x \hat{y}] e^{-jkz} \quad (1.2)$$

The polarization of a wave is always determined by the characteristics of the  $\mathbf{E}$  field and can be described in terms of a desired co-polar component  $E_{co}$  which is parallel with the co-polar unit vector  $\hat{c}o$ , and an undesired cross-polar component  $E_{xp}$ , which is parallel with a cross-polar unit vector  $\hat{x}p$ , which is orthogonal to  $\hat{c}o$ . Both  $\hat{c}o$  and  $\hat{x}p$  are orthogonal to each other and to the direction of propagation  $\hat{z}$ . Thus we can write the total  $\mathbf{E}$  field as

$$\mathbf{E} = [E_{co} \hat{c}o + E_{xp} \hat{x}p] e^{-jkz} \quad (1.3)$$

The co and cross-polar components of the  $E$  field ( $\mathbf{E}_t$ ) can be found by scalar multiplication of the  $E$  field with  $\hat{c}o^*$  and  $\hat{x}p^*$  respectively, i-e

$$E_{co} = \mathbf{E}_t \hat{c}o^* \quad E_{cp} = \mathbf{E}_t \hat{x}p^* \quad (1.4)$$

### 1.2.1.1 Linear Polarization

Considering the wave propagation along the z-axis, the polarization is called linear if the tip of the E field vector oscillates on a straight line within the X-Y plane perpendicular to the transmission direction. When the E field is y-directed, we term it as linearly y-polarized and is given by

$$\hat{c}o = \hat{y} \quad \hat{x}p = \hat{x} \quad (1.5)$$

$$E_{co} = \mathbf{E}_t \hat{y}^* = E_y \quad (1.6)$$

$$E_{xp} = \mathbf{E}_t \hat{x}^* = E_x \quad (1.7)$$

Generally an arbitrary linear polarization can be defined by co and cross-polar unit vectors of the form

$$\hat{c}o = \cos \xi \hat{x} + \sin \xi \hat{y} \quad (1.8)$$

$$\hat{x}p = \sin \xi \hat{x} - \cos \xi \hat{y} \quad (1.9)$$

or We see that  $\xi = \pi/2$  for a desired y-polarization and  $\xi = 0$  for a desired x-polarization.[6]

### 1.2.1.2 Circular Polarization

The  $E$  field vector of a circularly polarized wave propagates along a circularly helix in the direction of propagation. This polarization is called RHC or LHC depending if its rotation in clockwise or counter clockwise respectively. The RHC polarization is defined by the unit vector

$$\hat{c}o = [\hat{x} - j\hat{y}] / \sqrt{2} \quad (1.10)$$

which means that the y-component has a phase factor  $-j = e^{-j\frac{\pi}{2}}$  compared to x-component. In other words the y-component is delayed by quarter of a period. A RHC-polarized plane wave has the form

$$E = \hat{c}o e^{-jkz} = [\hat{x} - j\hat{y}] e^{-jkz} / \sqrt{2} \quad (1.11)$$

Detailed analysis of circular polarization can be reached in [6].

### 1.2.2 Axial Ratio

The quality of circular polarization is defined by its *axial ratio* and *cross polar isolation* performance. For a desired circular polarization the axial ratio (AR) in *dB* and the amplitudes of the co-and cross-polar fields are related by

$$AR_{dB} = 10 \log \left[ \frac{|E_{co}| + |E_{xp}|}{|E_{co}| - |E_{xp}|} \right]^2 \quad (1.12)$$

For an ideal circular polarization the *axial ratio* is unity (*0dB*)

### 1.2.3 Cross Polar Isolation

The cross-polar level can be described in four different ways as classified in [10], out of which I will present it as

$$XP_{dB} = 10 \log \left| \frac{E_{xp}}{E_{co}} \right|^2 \quad (1.13)$$

The relative cross-polar isolation must be ideally 0 ( infinite *dB*)

### 1.2.4 Return Loss

Return loss is the measure of input reflections from an electrical port of a microwave device. In common microwave designs a return loss of better than 15dB is usual, however a return loss better then 20dB over most of the operating band is more desirable. A return loss better than 30dB is required for this OMT design.

### 1.2.5 Isolation

The isolation between the output ports of an OMT is the main criteria in defining OMTs performance. Transmitting signals contains much more power as compared to the received signal; therefore if good isolation is not present between the output ports, the transmitting signal can severely damage the receivers input circuitry. Isolation better than 30dB is thus usually required when dual polarization is introduced. Since two orthogonal polarizations are to be transmitted, the two transmitted signals must be well separated and incoherent to each other. An isolation better than 35dB for the overall device is required for this project.

The design of orthomode transducer has been well described theoretically as well as practically in the following chapters. Each chapter is dedicated to individual component that has been theoretically studied and designed for this OMT project.

## Chapter 2

# Orthomode Transduce (OMT)

An Ortho-mode transducer (OMT) is an essential component in feed systems where frequency reuse is adopted, e.g. in satellite antennas and earth stations. An OMT is a polarization filter which separates two orthogonal polarizations within the same frequency band. Two frequency channels can then be used simultaneously, which enhances system capacity.

In general, an ordinary OMT is electrically a four port device, though it exhibits only three physical ports. The common port is usually of a square or circular cross section (interfacing the feed horn), provides two electrical ports that are allocated to the independent orthogonal dominant modes ( $TE_{10}$  and  $TE_{01}$ ) for square waveguide and ( $TE_{11}/TE_{11}$ ) for circular waveguide respectively. The remaining two ports are formed by standard waveguide or coaxial ports, serving the respective fundamental single signal mode only.

The OMT's are required to discriminate two orthogonal polarized dominant modes provided at the common port, usually interfaced with the feed horn, and supplying them to the single signal interface ports while maintaining a good match at all electrical ports and high cross polarization discrimination between the orthogonal modes. The scattering matrix of an ideal OMT is

$$\begin{bmatrix} 0 & 0 & e^{j\phi_1} & 0 \\ 0 & 0 & 0 & e^{j\phi_2} \\ e^{j\phi_1} & 0 & 0 & 0 \\ 0 & e^{j\phi_2} & 0 & 0 \end{bmatrix}$$

Ports 1 and 2 in Fig.2.1[7], represents the single signal fundamental mode ports, whereas the the third physical common port is formed by the electrical ports 3 and 4. The S matrix can be well understood by observing the Fig. 2.1. Connections are provided between ports 1 and 3; ports 2 and 4 respectively. The excitation of higher order modes

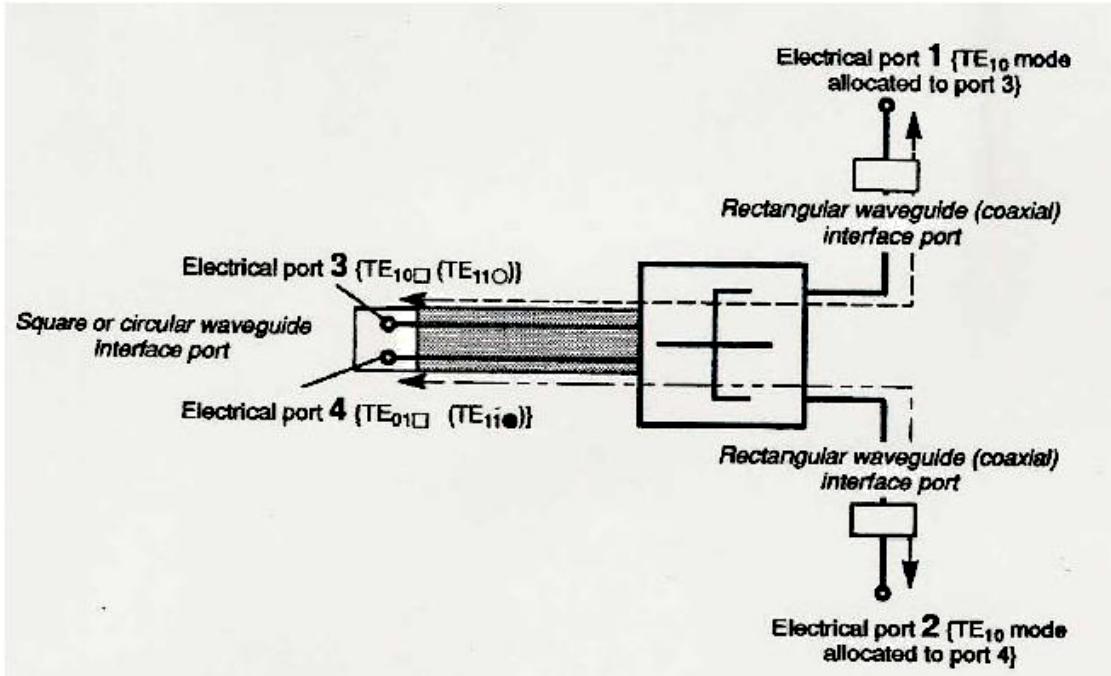


FIGURE 2.1: Principle equivalent circuit of an OMT.

(due to discontinuities present in the structure) badly affect the match and isolation performance of an OMT design, especially within the physical branching region. It should be considered that such unwanted higher order modes could also affect the radiation pattern of the antenna. A careful definition of the common port cross section and using symmetries in the structure reduces the generation of higher order modes to a certain extent.

Considering arbitrary discontinuities within a waveguide, the electromagnetic ( $EM$ ) fields that are excited by a dominant mode may be regarded as the series expansion of all possible dominant and higher order modes. The EM fields inside a rectangular waveguide can be expressed as the superposition of all higher order waveguide modes.

$$EM = \sum_{m=1}^k TE_{m0} + \sum_{m=0}^k \sum_{n=1}^k TE_{mn} + \sum_{m=1}^k \sum_{n=1}^k TM_{mn} \quad (2.1)$$

Most commercial applications concerns narrow band designs in which all higher order modes of the common waveguide are evanescent within the operating band. As a result, these modes only influence the field propagation near to the discontinuity and are therefore called *localized modes*. However these higher order modes couplings may cause isolation impairments in wideband applications. These higher order modes are called *accessible* because they propagate as their cut-off frequencies become lower than operating frequencies of the upper band edge.

An appropriate symmetrical design of the required discontinuities, e.g. matching sections, junctions and the septum provides the suppression of higher order modes in an OMT. We know that, the dominant mode only excites the special  $TE_{mn}/TM_{mn}$  mode types at steps or probes that are symmetrical to both the waveguide planes.

$$\sum_{m=1}^k \sum_{n=0}^k TE_{(2m-1)(2n)} \quad (2.2)$$

$$\sum_{m=1}^k \sum_{n=1}^k TM_{(2m-1)(2n)} \quad (2.3)$$

If discontinuities show symmetry along the  $X$  axis, the excited  $TE_{mn}$  and  $TM_{mn}$  modes can be represented by the following equations respectively.

$$\sum_{m=1}^k \sum_{n=0}^k TE_{(m)(2n)} \quad \sum_{m=1}^k \sum_{n=1}^k TM_{(m)(2n)} \quad (2.4)$$

However if discontinuities show symmetry along  $Y$  axis alone, the dominant modes excites the special mode types

$$\sum_{m=1}^k \sum_{n=0}^k TM_{(2m-1)(n)} TE_{(2m-1)(n)} \quad \sum_{m=1}^k \sum_{n=1}^k TM_{(2m-1)(n)} \quad (2.5)$$

To obtain the required performance without impairments, the mode properties should be considered before designing the OMT structure. A detailed discussion on the theory and CAD for designing OMT's can be reached in [7]

The OMT under discussion has been designed in the gap waveguide technology, rather using the standard waveguide technology, to study if it is realizable and better in terms of its electrical performance as compared to existing standard waveguide based alternatives. The final device has been obtained in three major steps that includes gap waveguide, septum polarizer and the quarter wave plate, which have been discussed in detail in the subsequent chapters.

## Chapter 3

# Gap Waveguide

This chapter presents a newly introduced metamaterial based waveguide technology known as *ridge gap waveguide*[1]. The gap waveguide is formed inside the gap between the two parallel metal plates, one of which is provided with a texture or thin multilayer structure. The texture is used to realize some kind of a high impedance surface, which might ideally be a PMC surface, surrounding a conducting ridge. The ridge gap waveguides are believed to have much lower losses, and are much cheaper to manufacture since they are planar in nature as compared to hollow waveguides. The transmission line analysis related to microstrip lines is almost applicable to ridge gap waveguides as a good approximation, by introducing analogies with microstrip lines, but only within the operating bandwidth in which the PMC realization creates cut-off for waves propagating in direction other than along the conducting ridge.

The gap waveguides do not require additional packaging as compared to the severe packaging issues related to microstrip circuits, since the gap waveguides are completely shielded by metal, which is also the basis for its low losses and good electrical performance. A detailed discussion has been carried out in the following sections particularly highlighting the need to introduce such a waveguide technology, its design, working principle and various advantages.

### 3.1 Introduction

Hollow rectangular waveguides are mostly used to realize components for frequencies between 3 to 30 *GHz*, however with increasing the operating frequency further, the waveguide dimensions become smaller which in turn introduces manufacturing limitations. At higher frequencies, when the waveguides are required to be manufactured in two parts which can be joined together, requires ensuring very good electrical contact in the joints. This is usually achieved by putting more screws to avoid leakage of electromagnetic energy at smaller wavelengths typically at millimeter and submillimeter wavelengths. For

wideband applications, microstrip lines are used as well but they offer more losses at higher frequencies with additional reduction in the power handling capability. Therefore new waveguides or transmission lines are required to operate at higher frequencies particularly above 30 GHz. The so called *substrate integrated waveguide* (SIW) already exists for used at higher frequencies, but these waveguides still suffer from losses due to the substrate and the metalized via holes that represents a complicated and expensive structure to manufacture.

### 3.2 High Impedance Surfaces

The electromagnetic properties of a conducting surface can be altered by incorporating a special texture on the surface which helps in describing the surface with a single parameter termed as its surface impedance. Magnetic conductivity does not exist naturally but can be realized in the form of high surface impedance. The first conceptual attempt to realize high surface impedance was the so called *soft* and *hard* surfaces [8], where they were defined in terms of their anisotropic surface impedance.

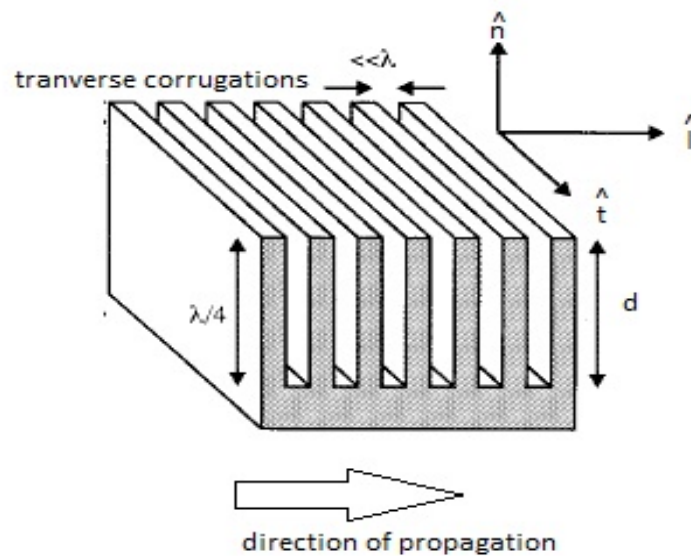


FIGURE 3.1: Transversely corrugated soft surface

Fig.3.1 describes a transversely corrugated soft surface with two principal directions both being tangential to the surface: the longitudinal direction  $\hat{l}$  which is in the direction of the pointing vector and the transverse direction  $\hat{t}$  orthogonal to it. The longitudinal and transverse surface impedances are given by

$$Z_l = -\frac{E_l}{H_t} \quad \text{and} \quad Z_t = -\frac{E_t}{H_l} \quad (3.1)$$

From the knowledge of transversely corrugated surfaces we can uniquely define a soft surface by

$$Z_l = 0 \quad \text{and} \quad Z_t = \text{infinity} \quad (3.2)$$

In principle the soft surfaces acts as shorted transmission lines for the longitudinal polarizations and transform the short to infinite impedance at the aperture of the corrugations, when the slot depth  $d$  equals a quarter wavelength. If we consider a poynting vector in  $l^\wedge$  direction along the surface, we can have two orthogonal components, one being tangential( $E_t$ ) to the surface and the other orthogonal( $E_n$ ) to the surface. They are both zero at the soft surface so that the poynting vector is zero at the soft surface.

$$E_t = E_n = 0 \quad (3.3)$$

A grid of parallel PEC / PMC strips, where every second strip is PEC and PMC respectively [4] is used now a days to describe the ideal soft and hard surfaces. They are characterized by their *anisotropic* boundary conditions, that allows an arbitrary polarized wave to propagate along the strips (hard surface case) whereas they stop wave propagation in directions orthogonal to the strips (soft surface case). High impedance surfaces with a forbidden frequency band have been discussed in detail in [9]. Due to the *isotropic* boundary conditions, the *EBG* surface [9] stops wave propagation in all directions. *Fakir's bed of nails* refers to a two dimensional array of metal pins [3] arranged on the conducting surface, which mimic the ideal impedance surface boundary. It has been demonstrated in [10], that by placing the structure in between two parallel plates and varying different parameters typically the gap height, can produce extremely large banggap (parallel palte stop band)(2.5:1) to prevent wave propagation. The surface impedance is very high in the bandgap, so the tangential magnetic field is small, even with a large electric field along the surface. Such a structure is sometimes described as a *magnetic conductor*.

### 3.2.1 PMC Realization Using Bed of Nails

In fact there are many ways of realizing parallel plate stop band, which have been compared in [11], but gap waveguides introduced in [1] and experimentally verified in [2] have made use of bed of nails [3], as a high impedance surface for parallel plate mode suppression. Fig. 3.2 has been taken from [12] in order to motivate the need for using bed of nails as a high impedance surface in gap waveguide technology. The 2-D colour plots show the suppression of different cavity modes as well as the strong fields in the bends of the microstrip line within the stop band(*Octave bandwidth*) when the lid of nails is employed. It can be observed that the mode suppression has a bandwidth of more than 2:1 and it does not interfere much with the microstrip circuit. Therefore this

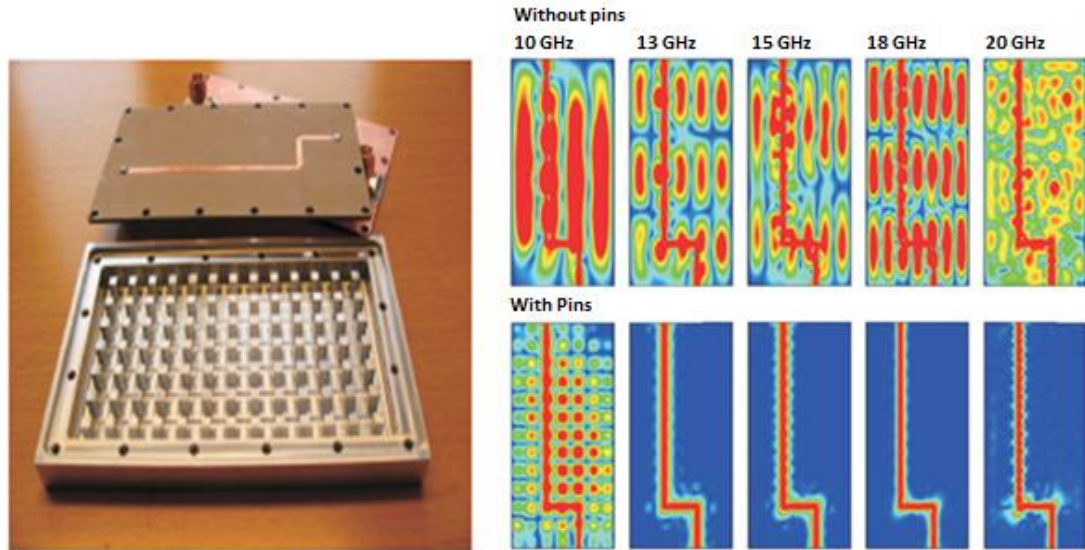


FIGURE 3.2: Manufactured metal lid with pins (left), 2-D color plots of vert. E field distribution (right) inside the gap between the microstrip board and the lid of the metal box, both (a) with smooth metal lid and (b) with a lid of nails.

mode suppression technique has introduced a new advantageous packaging technology for high frequency circuits.

The metal pins can be easily milled in the same way as the conducting ridge can be. Such manufacturing allows to vary the height of the texture, thereby providing more degrees of freedom in a design process than substrate bound alternatives. Furthermore it is believed that it is possible to integrate active and passive components like amplifiers and MMIC's even in the form of unpackaged semiconductor chips, which should be easy because the metal pins may also work as heat sink, provide cooling, shielding and packaging at the same time. A comparative study for investigating the PMC realizations [11], has motivated the need to use bed of nails approach, providing band stop for more than an octave band, furthermore this technology is less lossy, cheap and easy to mill.

### 3.3 Ridge Gap Waveguide

The propagation characteristics along soft and hard surfaces are very well known, either when they are introduced in hollow waveguides or as open hard and soft surfaces.[4]. The detection of local surface waves along each groove of a hard surface, introduced in[13], has been followed by the detection of local modes along the ridges of a longitudinal corrugated hard surface, when a smooth metal plate, separated by a narrow gap was located over it[14]. This has resulted in a new way of killing higher order modes[14], by introducing the hard surface in a TEM parallel-plate waveguide. The geometry in [14] has been simplified and improved in [1] to introduced a new basic waveguide confined in the gap between parallel plates.

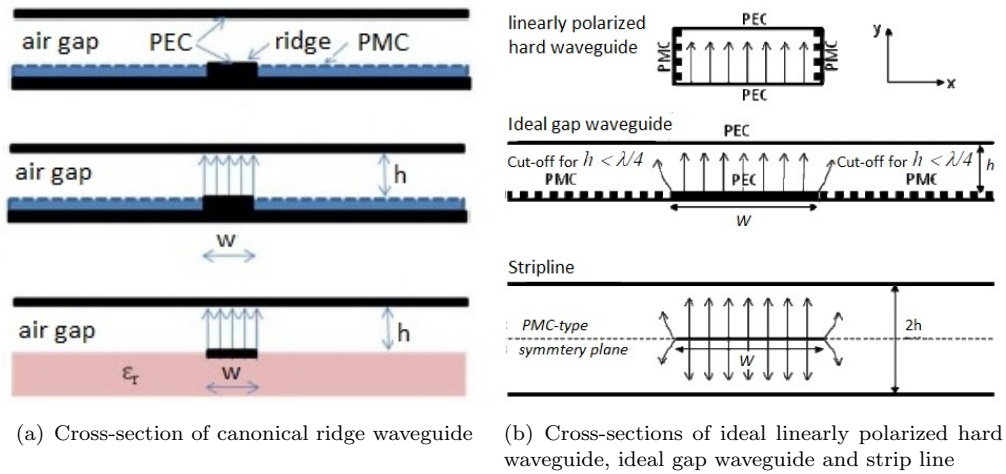


FIGURE 3.3: Cross-sectional views of ideal gap waveguide and its similarities with other transmission lines

### 3.3.1 Physical Theory

The basic concept of the ridge gap waveguide has been comprehensively discussed in the earlier sections. The geometry in Fig.3.3(a) shows a ridge surrounded by PMC surface on both sides of the ridge. The propagation of the TEM waves in any arbitrary direction without any low frequency cut-off, guided between two smooth parallel metal surfaces, are called *global parallel plate modes* in the sense that they fill the gap, whereas the quasi-TEM waves of the ridge gap waveguide follows only the conducting ridge, hence called *local waves*. When the spacing between the smooth parallel metal surfaces is less than a quarter wavelength, only the global TEM waves propagate between them, which in turn can destroy the local gap waveguide performance completely. These propagation of these global parallel plate modes is very critical for the gap waveguide performance. The high impedance surface on both sides of the ridge provides cut-off for the global parallel plate modes.

### 3.3.2 Principle of Operation

The principle of operation of the gap waveguide is based on the following theoretical facts that are either well known or can readily be derived from Maxwell's equations:

- If the gap height ' $h$ ' between a PEC and a PMC surface is less than a quarter wavelength, the wave propagation becomes prohibited in any arbitrary direction.
- Wave propagation in any direction can be made prohibited, in between a PEC and an EBG surface if the gap height is typically small. This gap height depends upon the geometry of the EBG surface and it is found to be less than a quarter wavelength as well. Most practical EBG surfaces work as an artificial PMC for all

angles of incidence in the elevation plane for the vertical polarization (i-e  $TM_n$  case with respect to the surface normal). For horizontal polarizations (i-e  $TE_n$  case) with normal incidence, the EBG surfaces act as a PMC and as a PEC for grazing incidence. It is this property that provides the bandgap for horizontal polarizations. The PEC boundary conditions between the parallel plates for horizontal polarization provides cut-off whenever  $h < \lambda/2$ , which is a weaker cut-off condition than  $h < \lambda/4$ , which is valid for the PMC boundary condition on the lower plate.

- Waves in the gap between a PEC surface and a PEC/PMC strip grid can only propagate along the direction of the PEC strips whereas they are in cut-off for vertical( $TM_n$ ) and horizontal( $TE_n$ ) polarization when  $h < \lambda/4$  and  $h < \lambda/2$  respectively. Therefore an ideal gap waveguide works for all frequencies up to a maximum defined by  $h = \lambda/4$ .

The bandwidth of the propagating wave along the ridge can be estimated from the frequency band over which the propagation constant in directions away from the ridge is imaginary, corresponding to an evanescent wave. For the special bed of nails EBG surface used in [1], the PMC appears ideal for thin pins and small periods when the pin length  $d = \lambda/4$  and the bandgap is at high frequency limited by a  $TE_n$  wave starting to propagate when  $d+h = \lambda/2$ . From the comparative studies of [11], it was possible to design gap waveguides with octave bandwidth (2:1).

Fig.3.4 has been taken from [1] showing the dispersion diagrams for the gap waveguide to justify the above discussion related to its band stop characteristics. The dispersion diagrams in Fig.3.4(a) and Fig.3.4(b) were computed without ridges for infinite periodic structure and finite dimensions in transverse plane with PEC side walls respectively, showing a large stopband above 10 GHz where no waves can propagate. The basic parallel plate mode that started at zero frequency as a TEM mode, is represented by the left curve in Fig.3.4(a). This mode is then deviated from the light line and went into cut-off just below 10 GHz. It appeared again at 23 GHz together with another mode. Several rectangular waveguide modes appeared below 10GHz, when metal walls were introduced, limiting the transverse extent of the parallel plate geometry in Fig.3.4(b). These modes have a lower cut-off similar to a normal rectangular waveguide modes but went into a stop band just below 10 GHz and appeared again at the end of this parallel plate stop band at 21 GHz. The dispersion diagram of Fig.3.4(c) includes the ridge as well. The diagram which relates the introduction of the ridge, shows a new mode propagating closely to the light line, in fact following the ridge within the whole parallel plate stopband. This is the desired quasi-TEM mode and it is termed as quasi-TEM because it follows the light line very closely but not exactly. Another higher order gap waveguide mode appeared at 19 GHz, having a vertical E field distribution with asymmetrical sinusoidal dependence across the ridge, being zero in the middle of the ridge.

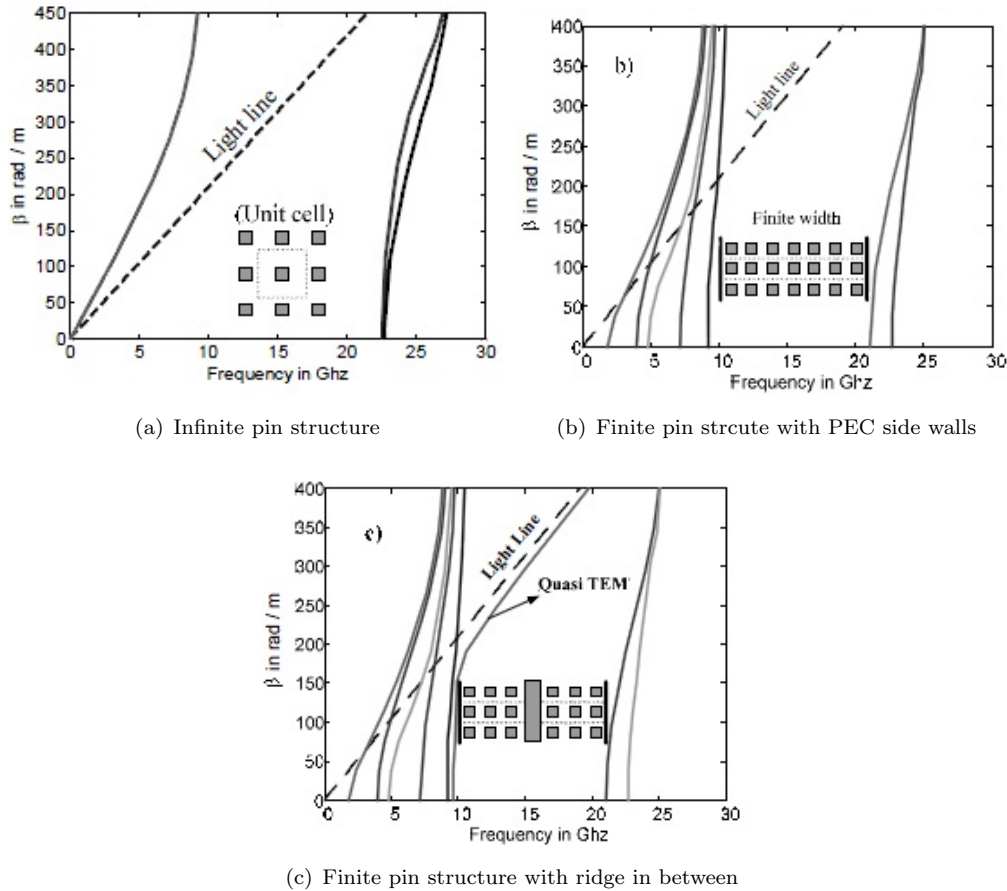


FIGURE 3.4: Dispersion diagram for the gap waveguide

### 3.3.3 Similarities With Other Transmission Lines & Waveguides

The gap waveguide has similarities with several other transmission lines and waveguides. It can be considered as a linearly polarized hard waveguide Fig.3.3(b) consisting of two horizontal PEC and two vertical PMC walls, that supports a uniform TEM field. The *ideal gap waveguide* in Fig.3.3(b) is confined between two parallel surfaces, one being PEC and the other PMC with a guiding PEC strip in the PMC plate that guides the propagation of TEM mode while the PMC region on both sides of the PEC strip provides cut-off for parallel plate modes, when the gap height  $h < \lambda/4$ , which shows similarity with the hard waveguide.

There is an exponential field decay in all directions away from the PEC strip, in a similar way as the propagating field in a hard waveguide penetrates into all type of hard wall realizations. The ideal linearly polarized hard waveguides can be miniaturized like the gap waveguide, which means that the gap waveguide has no lower cut-off related to its width ' $w$ ' and gap height ' $h$ ', as long as the parallel-plate cut-off has been realized. Geometrically the gap waveguide looks similar to an inverted microstrip line Fig.3.3(a) where the substrate is suspended above the ground plane to make the waves propagation over the strip, in the air gap between the strip and the substrate. The strip line in

Fig.3.3(b) consist of parallel metal plates separated by a substrate with a metal strip halfway between the parallel plates. The strip line has a PMC type symmetry plane in the middle of the gap as illustrated, which makes it look like two opposing gap waveguides, one being an image of the other.

### 3.3.4 Designing For Desired Characteristic Impedance

It has been established in [1] and [2] that within the operating fequency band in which the artificial surface works as a PMC, many of the microstrip line equations can serve as a good approximation for the ridge gap waveguides based on the similarities of ridge gap waveguides with the microstrip line structures of Fig.3.3. By applying an approximation  $w \gg h$  in the same way as for microstrip line, the characteristic impedance of the gap waveguide is given approximately by that of a microstrip line

$$Z_k = Z_o h/w \quad (3.4)$$

where  $Z_k$  is the wave impedance in air, ' $w$ ' is the width of the ridge and ' $h$ ' is the gap height. The propagation constant will be the same as in air. For ideal gap waveguide an approximation for the characteristic impedance given an ideal PMC case would actually be to use twice the characteristic impedance of a stripline.

$$Z = 2Z_{stripline} \quad (3.5)$$

where  $Z_{stripline}$  can be found in [15] to be

$$Z_{stripline} = \frac{\eta}{4} \left( \frac{W_e}{2h} + 0.441 \right)^{-1} \quad (3.6)$$

with

$$\frac{W_e}{2h} = \frac{W}{2h} - \begin{cases} 0 & \text{if } \frac{W}{2h} > 0.35, \\ (0.35 - \frac{W}{2h})^2 & \text{if } \frac{W}{2h} < 0.35. \end{cases} \quad (3.7)$$

This formulae provides a quick estimate but unfortunately it may not be much accurate when PMC realization is considered in practice, therefore methods have been described in [1] to calculate or approximate the desired characteristic impedance for the ridge gap waveguide.

## 3.4 Analysis

The major advantage, the ridge gap waveguides have over hollow waveguides is that they are planner and much cheaper to manufacture, particularly at high frequencies

such as for millimetre and sub millimetre waves. The latter is due to the fact that ridge gap waveguides do not require very good electrical contact between the parallel plates. The wave propagation is suppressed in any arbitrary direction other than the desired path (conducting ridge) by making use of the PMC realization, which makes it easy to apply mechanical joints far away from the propagation path. Bed of nails [3] has been employed to realize the PMC surface. The metal pins can be easily milled in the same way as the conducting ridge can be. Such manufacturing allows to vary the height of the texture, thereby providing more degrees of freedom in a design process than substrate bound alternatives. Furthermore it is believed that it is possible to integrate active and passive components like amplifiers and MMIC's even in the form of unpackaged semiconductors chips, which should be easy because the metal pins may also work as heat sink, provide cooling, shielding and packaging at the same time.

All these facts have motivated the need to explore gap waveguide technology in terms of realizing its manufacturing feasibility and its electrical performance by designing waveguide components for THz. This orthomode transducer is among the passive components that are in pipeline for design and investigation. The OMT design has been comprehensively presented in the following chapters.

## Chapter 4

# Septum Polarizer

### 4.1 Introduction

A circular polarized wave is represented by the superposition of two orthogonal linearly polarized waves that possess equal magnitude and a quadrature phase difference. For dual linear operation, an antennas feed system would serve a 3 *dB* portion of a circularly polarized signal at the interface ports allocated to the respective polarizations. Therefore only one circularly polarized signal could be received by such a feed system, introducing a loss of 3 dB since the semi signals of RHCP and LHCP are supplied at the identical ports.

Consequently, additional components must be incorporated to facilitate the circular polarization operation of a feed system, so that appropriate transformation of linearly polarized signals into the circularly polarized signals, received from or transmitted to the antenna interface port, without any systematic loss. The equipment will additionally provide discrimination of RHCP and LHCP signals to allow frequency reuse of the available frequency bands.

There are two principle methods for the generation and discrimination of circularly polarized signals. Firstly, conventional polarizer can be connected to the common port of the feed system, secondly a circuitry of components properly interconnected with the single signal ports of an OMT.

### 4.2 Operation

The septum polarizer is electrically a four port but physically a three port passive waveguide device illustrated in Fig.4.1 which have been taken from [16] and [6].The common port of the square waveguide constitutes two electrical ports representing two orthogonal

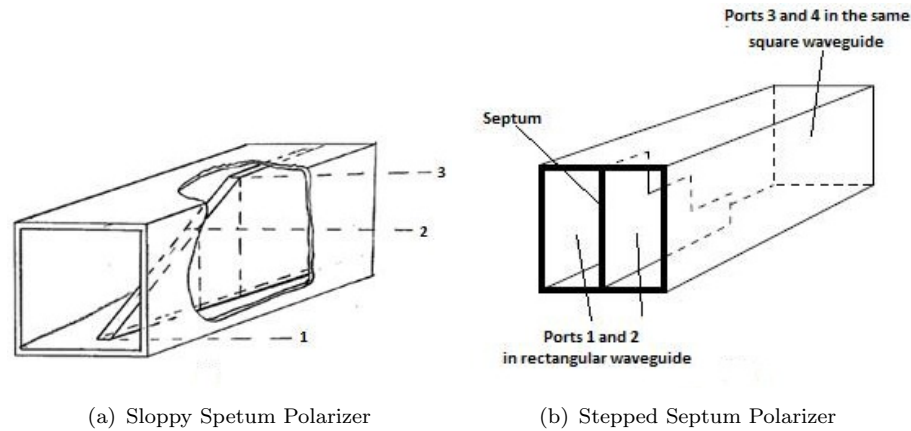


FIGURE 4.1: Common type of septum polarizers.

modes as shown in Fig.4.1(b). A sloppy Fig.4.1(a) or stepped septum Fig.4.1(b) divides the square waveguide into two standard rectangular waveguides sharing a common broad wall.

A signal supplied to each of the standard rectangular waveguide port is transformed into a RHCP or LHCP respectively, conversely a circularly polarized signal depending upon its sense, e.g. RHCP or LHCP propagating in the square waveguide towards the septum couples to only one of the rectangular ports. The operation of the septum polarizer is illustrated in Fig.4.2. The septum may have a continuous (sloppy) or stepped shape over its length. The design of the septum region is very critical for proper polarizer functionality, for instance power splitting (combination) and a  $+/- 90^\circ$  differential phase shift. The energy of the circularly polarized is distributed in two orthogonal components,  $TE_{10}$  and  $TE_{01}$ , one normal to the septum and the other parallel to the septum. The normal component simply divides in half as it travels down the septum region. Observe the phase vectors in Fig.4.2, taken from [16], are in the same direction, i.e. transformed into two even mode signals. The parallel component on the other hand remains perpendicular at the walls of the septum. By the time the energy reaches the end of the septum (in the rectangular waveguide), the phase vectors are back to back, i.e. transformed into two odd-mode signals.

#### 4.2.1 Even-Mode Excitation

The even mode excitation can be further explained by the fact that, when an even mode is excited in the rectangular waveguide region, the electric currents on each side of the common wall flow in opposite directions however the electric and magnetic field are distributed identically in the right and left rectangular waveguides. Therefore a slot in the common wall will not disturb the fields and current flow in one guide, as it will be the return current of adjacent guide through the slot. As a result the even mode will be

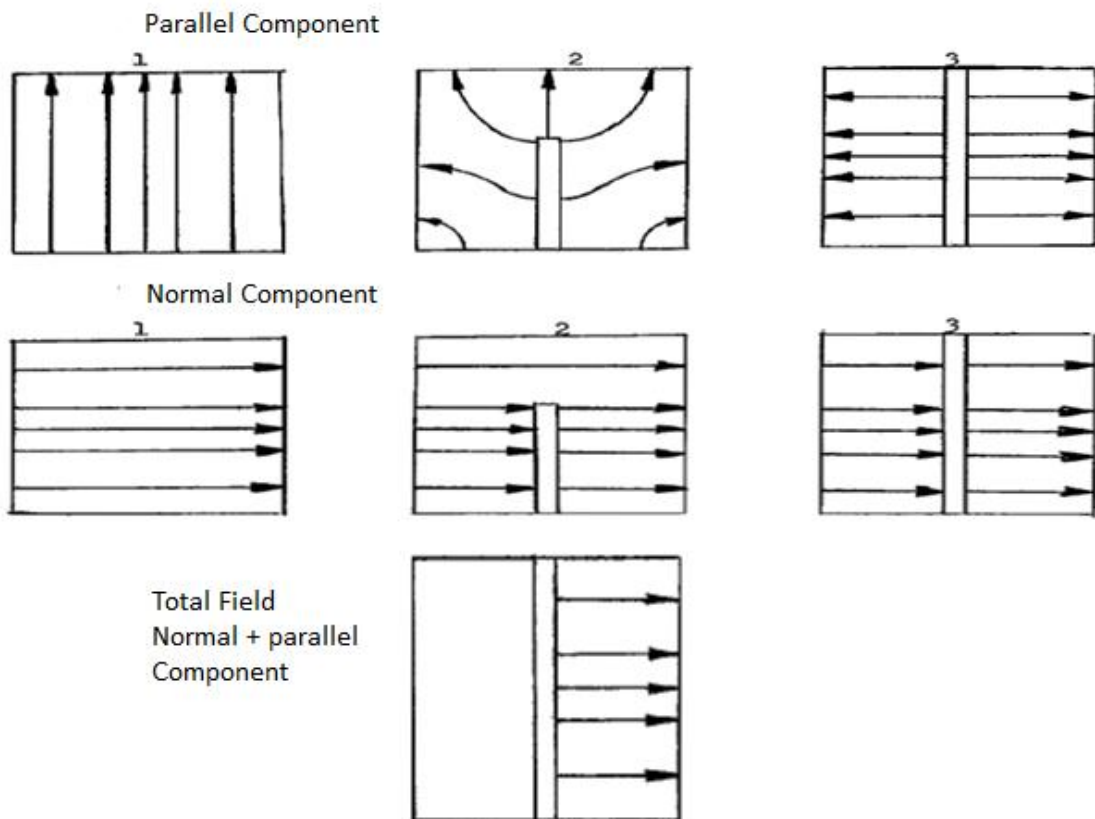


FIGURE 4.2: Propagation of parallel component (top) followed by propagation of normal component (middle) and total E field (bottom).

unaffected by the septum and will transfer its total energy into the  $TE_{10}$  mode in the square waveguide.

#### 4.2.2 Odd-Mode Excitation

When an odd mode is excited in the rectangular waveguide region, the directions of the currents and the fields in the right and left rectangular waveguides are reversed in contrast to even mode case. This causes the current flow on either side of the common wall to be in the same direction, which will cause field disturbance, resulting in mode coupling and reflection, in case a slot is introduced in the common wall. The energy of the odd mode will be partially reflected and partially transferred to the  $TE_{01}$  mode in the common square waveguide section. This is due to the fact that the transverse field of an odd mode in a dual rectangular waveguide is characterized by odd symmetry on the left and right side whereas the  $TE_{10}$  mode in the square waveguide possessed an even symmetry, which leads to no coupling between them.

If both components with identical amplitudes and quadrature phase exists simultaneously, cancellation can occur in one of the rectangular ports, see figure above. Consider a

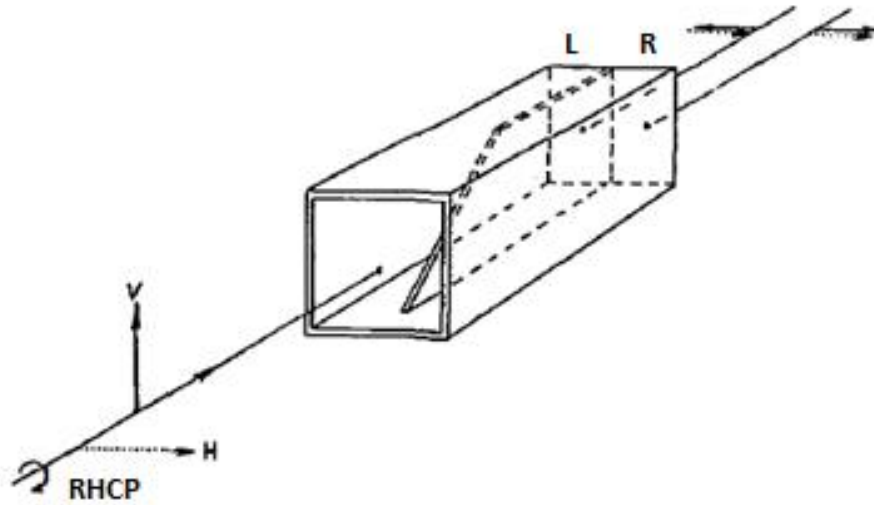


FIGURE 4.3: Polarization operation.

RHCP wave is propagating from the common port towards the septum, its two orthogonal components will be as shown in Fig.4.3, taken from [17], with the vertical component leading the horizontal by  $90^\circ$ . The septum will behave as a single ridge waveguide to the perpendicular component, which lowers the cut-off frequency hence the perpendicular component will propagate at a slower phase velocity than the horizontal component, which is unaffected by the septum.

This means that the guided wavelength for the vertical component is larger than the guided wavelength for horizontal component, hence the septum length appears to be longer for the vertical component, which results in a delayed component relative to the horizontal component of the input circular polarized signal. The septum must be designed carefully to give  $90^\circ$  differential delay, which makes the two resulting fields cancel completely in the rectangular port marked L, and add constructively in the port marked R, thus RHCP will couple only to the R port whereas the LHCP will couple to L. Conversely exciting port L will yield LHCP and port R will yield RHCP respectively.

### 4.3 Mathematical formulation

We can achieve perfect circular polarization if following conditions hold: For the first polarization

$$|S_{31}| = |S_{32}| \quad (4.1)$$

For the second polarization

$$|S_{41}| = |S_{42}| \quad (4.2)$$

Secondly a differential phase shift of  $+/- 90^\circ$  between these signals have to be accomplished, i.e.

$$\Delta\phi = \angle S_{31} - \angle S_{32} = +/ - 90^\circ \quad (4.3)$$

We can represent the polarizer as a passive four port device with the scattering matrix given by

$$S_{ij} = \frac{1}{\sqrt{2}} \begin{bmatrix} 0 & 0 & 1 & -j \\ 0 & 0 & -j & 1 \\ 1 & -j & 0 & 0 \\ -j & 1 & 0 & 0 \end{bmatrix}$$

To make the polarizer work, excite port 3 and port 4 with two equal but orthogonally X and Y polarized antennas, that must be impedance matched to the characteristic impedance of the ports, then from port 3 and port 4 they will excite a circularly wave of the form

$$Ee^{-jkz} = (V_3^m \hat{x} + V_4^m \hat{y})e^{-jkz} \quad (4.4)$$

where  $V_i^m$  are the signals going away from port  $i$

The quality of the circular polarization can be described in terms of its axial ratio and cross polar isolation, which has already defined by equation 1.1 and 1.2 respectively.

## Chapter 5

# Quarter Wave Plate

### 5.1 Introduction

There is always a great deal of discussion to choose specific polarization for specific applications. For a highly directional *line of sight* communication link, it's preferable to use linear (horizontal or vertical) polarization. However, the introduction of any scattering or reflection paths can significantly distort the polarization of the signal at the receiving station. In much application we need circular polarization which is immune to Faraday's rotation (depolarization of the linearly polarized signals due to noise in the channel).

This project relates to provide linear polarization; therefore we need to convert the circular polarization obtained after the stepped septum polarizer to linear polarization. At microwave frequencies, a very popular way is to use a waveguide that offers different propagation characteristics for the two orthogonal polarization vectors. The length of this waveguide is chosen such that one component is delayed by  $90^\circ$  with respect to the other component. A waveguide structure with these characteristics is called a quarter-wave plate.

### 5.2 Operation

Circular polarization consist of two orthogonal linearly polarized components, one delayed  $90^\circ$  with respect to the other. There are a number of ways to generate such circularly polarized waves. At low frequencies it is convenient to use two co-planner dipoles and feed them in quadrature phase, while at higher frequencies we rely on propagation delays to generate necessary phase shift instead of using phase shifters. As described above at microwave frequencies we use quarter wave plates, which can me designed by various means as well. I have analysed two major techniques:

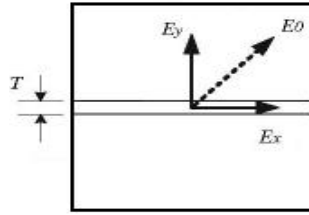


FIGURE 5.1: Incident wave decomposition inside a square waveguide.

A square waveguide was loaded periodically by thin capacitive or inductive irises in order to produce phase delay or phase advance respectively. When applied two fundamental modes to the square waveguide, the irises behaved inductively for one mode and capacitively for the other, thus it was made to produce an appropriate differential phase shift of  $90^\circ$ , which is used to convert linear to circular polarization and vice versa.

Another simple technique that has been adopted for this project was to insert a dielectric septum inside the square waveguide to realize circular or linear polarization. The dielectric septum behaves in the similar way and delays the parallel propagating mode relative to the normal one. Appropriate length and thickness can produce very good match between the ports and almost exact  $90^\circ$  of phase shift between the orthogonal modes. This design has the added advantage that by adjusting the length of the inserted dielectric septum, poor phase differences resulting from fabrication error or an inaccurate dielectric constant can easily be improved .

Figure.5.1 shows a typical square waveguide polarizer in which dielectric septum has been inserted in the middle of the waveguide. An incident wave oriented at 45 degrees relative to the dielectric septum will be decomposed into two identical orthogonal projections  $E_x$  and  $E_y$ , parallel and perpendicular relative to the septum respectively. Reflections would results in due to the discontinuity introduced by the septum region. A careful design of the septum can minimize these reflections to give a better match. We have designed a four step impedance matching transformer to maximally meet our return loss requirements.

Both of the orthogonal components will propagate with different propagation constants, since the horizontal component will be much effected by the septum as compared to the vertical one. Adequate septum length will produce  $90^\circ$  phase delay between the components, which in turn forms circular polarization. The length of the septum must satisfy

$$(B_x - B_y) \times L = 90^\circ \quad (5.1)$$

To determine the sense of circular polarization is always a bit tricky. The classic definition of RHCP is, when the polarization is rotating to the right with respect to the direction of propagation, and rotating to the left for LHCP. Normally we can use a helix

antenna, since a right handed helix radiates and receives RHCP and a left handed helix radiates and receives LHCP.

## Chapter 6

# Design & Simulation Analysis

The OMT has been designed and optimized in *Ansoft HFSS*. Initially I have analysed the performance of HFSS as compared to CST for an already designed standard waveguide OMT in CST operating at  $52GHz$ . HFSS has showed very close agreement with the results obtained from CST which has motivated the need to proceed the design in HFSS. As described above, the complete OMT has been designed in three steps, namely the gap waveguide, the stepped septum polarizer and the differential phase shifter. Adequate design details along with the simulated results have been discussed in the following sections.

### 6.1 CST vs HFSS Performance Analysis

The design details have been taken from an already designed standard waveguide OMT in *CST* at the Chalmers antenna group. The motive behind to redesign the same OMT in *HFSS* was to gain hands on experience on HFSS and to analyse the agreement between simulation results obtained from two different commercial softwares.

This OMT was designed to work between  $50GHz$  to  $56GHz$  with a return loss better than  $20dB$  and insertion loss better than  $0.1dB$ . The OMT has been shown in Fig.6.1 followed by its simulation results presented in Fig.6.2. The results have shown a very good agreement, even return loss for the vertical component and insertion loss for the horizontal component is better in HFSS than in CST. These results have formed good basis to develop our OMT design in HFSS.

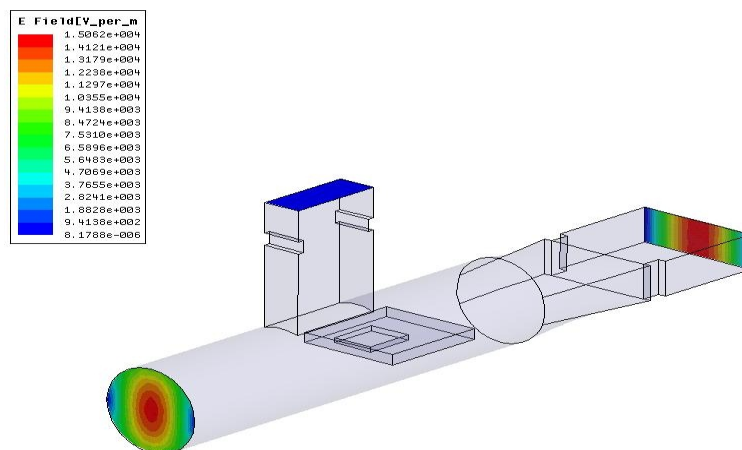


FIGURE 6.1: Standard waveguide based OMT, fabricated with aluminium, operating at (50 - 56) GHz band

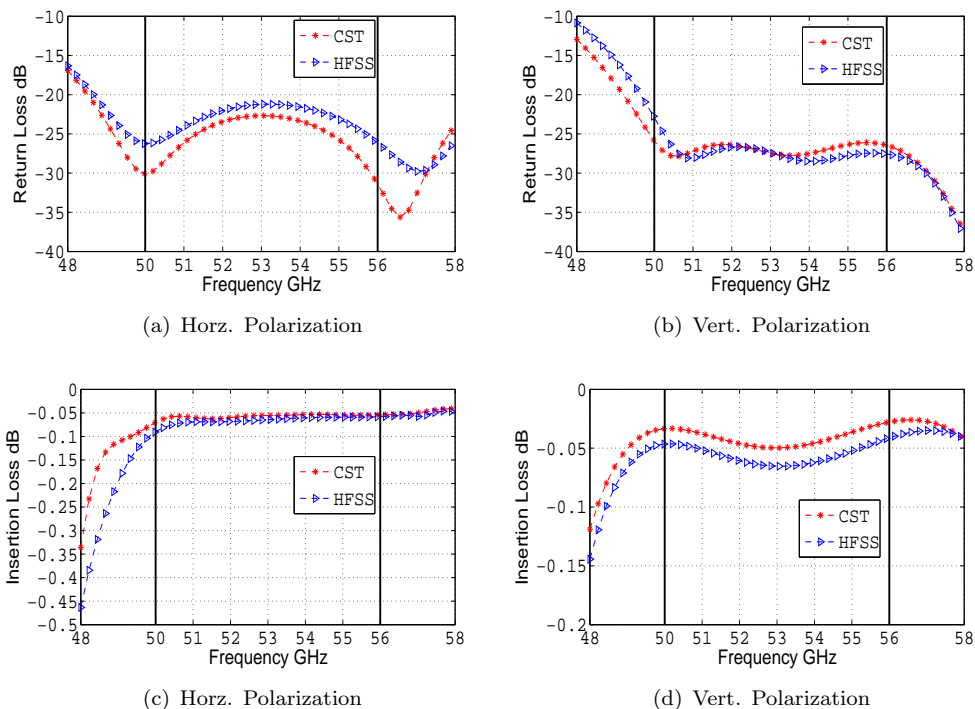


FIGURE 6.2: Return Loss and Insertion Loss Simulation Comparison

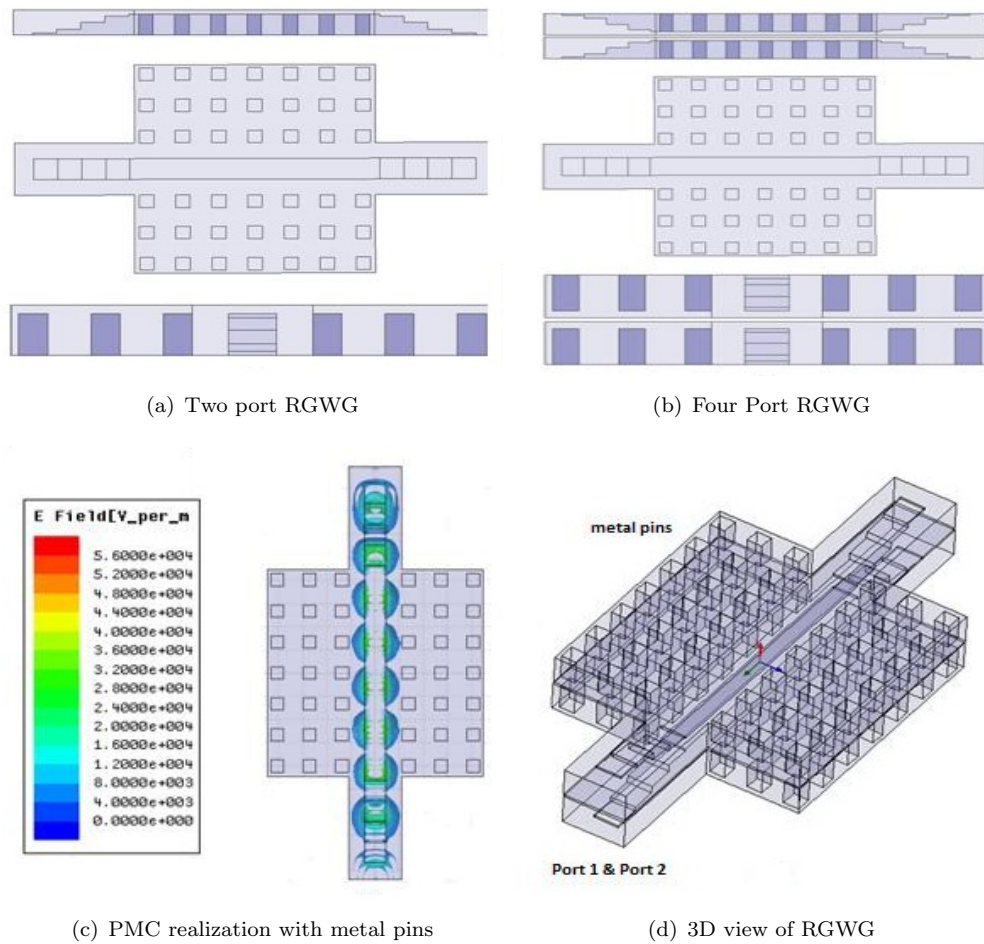


FIGURE 6.3: Ridge Gap Waveguide Geometry

## 6.2 Ridge Gap Waveguide

Initially it was proposed to design the whole structure for Ku band, and then the final design could be achieved by simple rescaling of the structure to the desired frequency band. Only rescaled and modified designs have been discussed in this report. The ridge gap waveguide dimensions have been taken from [2], and rescaled to the required frequency band.

The ridge gap waveguide has been duplicated and inverted on top of the first ridge gap waveguide, in order to obtain a four port structure. These ports will serve the fundamental / dominant mode for the respective waveguides which will propagate into the stepped septum polarizer to form circular polarization. The stepped septum polarizer will be discussed in the following section.

Four step impedance transformer has been designed and optimized to give minimum return loss, in other words, providing maximum match between the ridge gap waveguide and the standard rectangular waveguide ports. The return loss and the insertion loss

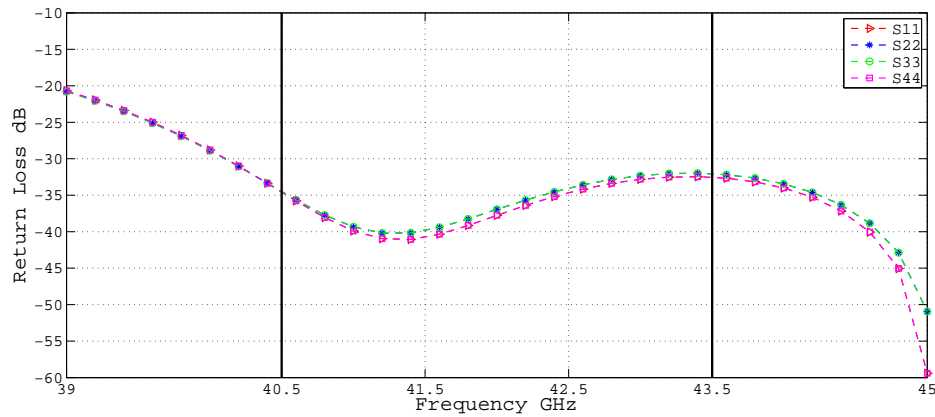


FIGURE 6.4: Return loss is below  $-30$  dB for approximately 12 percent bandwidth

for the optimized structure have been presented in Fig.6.4. It can be observed that the return loss for all the ports is below  $-30$  dB for approximately 12 percent bandwidth, which is greater than the required 7 percent bandwidth (see design requirements *section 1.1*). From Fig.6.3(c), it can be seen that, the metal pins have realized the PMC surface; hence no field is propagating in any direction except the conducting ridge. Furthermore both of the waveguides are also perfectly isolated.

The simulated return loss performance can be achieved over larger bandwidth, if more steps would have been introduced, but that will make the step dimensions hard to realize. The above results have fulfilled the initial design requirements and have provided means to proceed for further design objectives.

## 6.3 Septum Polarizer

Septum polarizers have been comprehensively discussed earlier in chapter 4. Initially it was proposed to design the septum polarizer using standard waveguide technology, which has resulted in acceptable performance, but later the design of septum polarizers in the gap waveguide technology has been realized, which has produced even much better electrical performance in terms of return loss and quality of circular polarization, than the existing standard waveguide based alternatives. The design of septum polarizers have therefore classified here in two ways, one based on standard waveguide technology and the other on the gap waveguide technology, which has been further classified with respect to the septum design, discussed in detail in the following sections.

### 6.3.1 Standard Waveguide Technology

The stepped septum polarizers [18] are known to have wide band characteristic as compared to sloppy septum polarizers [16]. The polarizer dimensions have been taken from

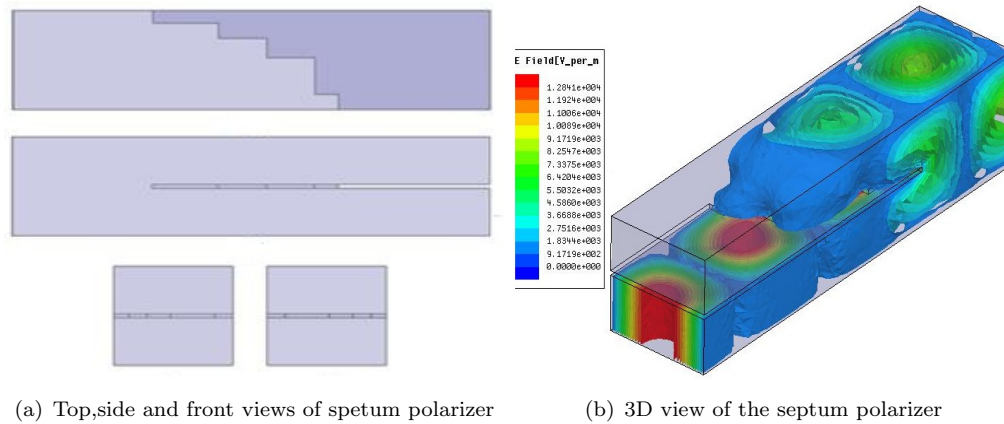


FIGURE 6.5: Septum polarizer in standard waveguide technology

[18], but have been optimized which has resulted in much better performance. Fig. 6.5(a) describes the top, side, front and bottom views of the septum polarizer. Fig. 6.5(b) is showing the electric field propagation when port 1 was excited, which resulted in RHCP, or conversely when port 3 was excited with RHCP, it had couple to port 1, providing good isolation from port 2 of the septum polarizer. LHCP can be obtained in the same way by exciting port 2 and vice versa.

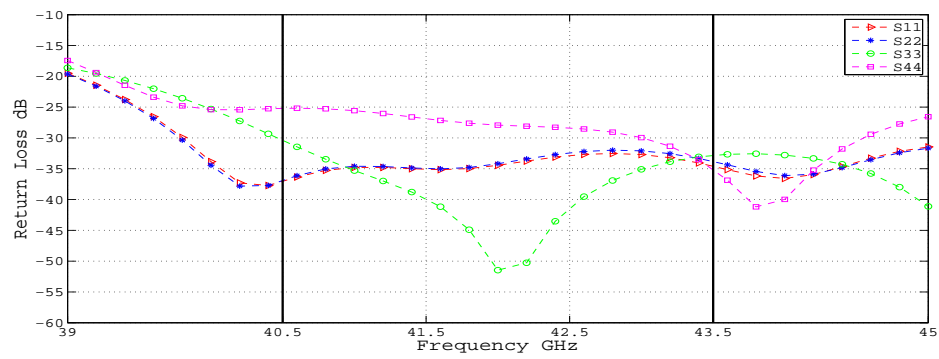
It can be observed in Fig. 6.6(a) that the device has yielded very good matching between all the ports maintaining an insertion loss of approximately  $3\text{dB}$ . This is due to the fact that the fundamental mode energy has been divided equally into two orthogonal components to yield good circular polarization.

The return loss for the horizontal component or  $TE_{01}$  mode has been a little poor than the vertical mode, which is due to the fact that the horizontal component of the circular polarization will more perturb by the septum, producing much reflections. Although it has been tried to optimize it as much as possible to meet the design requirements but it has been seen that there is a trade-off between the return loss and circular polarization performance.

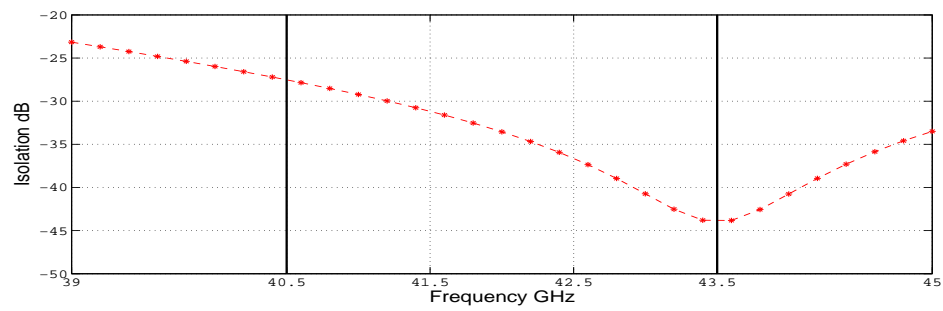
Improving the return loss degrades the axial ratio and hence the cross polar isolation. Although the design has been accomplished in HFSS but has been investigated with a commercial mode matching software, which has verified the results.

Similar reasons holds true for justifying the isolation performance of the device. Fig.6.6(b) describes the isolation between the fundamental mode ports of the septum polarizer, which is almost better than  $30\text{dB}$  for a reasonable bandwidth. Perhaps it is not fulfilling the design requirements, which needs it to be better than  $35\text{dB}$ , which is very much critical for satellite communication applications as well.

Fig.6.7(a) and Fig.6.7(b) describes that the polarizer has an axial ratio less than  $1\text{dB}$  and cross polar isolation better than  $24.5\text{dB}$ . The *MATLAB* code for analysing the axial

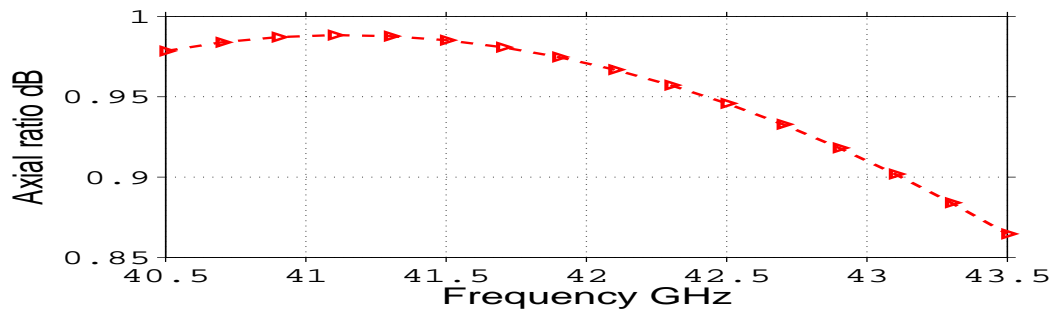


(a) Return Loss

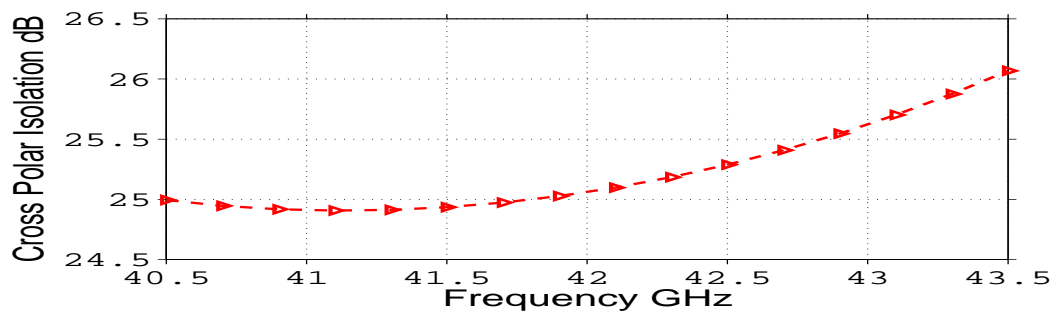


(b) Isolation

FIGURE 6.6: Return Loss and Isolation Performance



(a) Axial Ratio



(b) Cross Polar Isolation

FIGURE 6.7: Axial ratio and cross polar isolation for SWG septum polarizer

ratio and cross polar isolation can be found in *Appendix A*. Literature and past research contributions depicts the fact that the circular polarization performance can be improved even further, which usually requires a dielectric slab to improve the quadrature phase between the orthogonal components or alternatively introducing transverse corrugations followed by the septum, but that will definitely effect the insertion loss and return loss performance respectively, as it is always a trade off between improving the quality of circular polarization and the device's over all return loss performance.

### 6.3.2 Gap Waveguide Technology

The design of septum polarizer in gap waveguide technology has been studied in various ways, which includes the design using single layer and double layer pin texture, discussed in the following sections. Without the ridge, a gap waveguide is termed as a *groove gap waveguide*, which has been investigated in [19]. It has been concluded in [19] that the *groove gap waveguide* exhibits the same dispersion characteristics as of the ridge gap waveguide [2] however [19] has not compared the return loss performance with the ridge gap waveguide. It has however mentioned that there is strong  $E$  field penetration in the first row of pins in the *groove gap waveguide*, which I have found, is the main reason for the increase in return loss (5 to 10)  $dB$  of the *groove gap waveguide* with exactly same dimensions.

Varying various parameters to adjust the return loss performance, has resulted in the fact that halving the pin period can yield the same return loss performance as that of the ridge gap waveguide. An improvement of (7 to 15)  $dB$  has been observed over a wide frequency band, as shown in Fig.6.8. Therefore to maintain good electrical match between the ports, the septum polarizer in the gap waveguide technology comprises of half the pin period of the ridge gap waveguide pin period. However it has introduced unsymmetry in the design, if interfaced with the ridge gap waveguide. We should understand that the ridge gap waveguide has interfaced at the input of the septum polarizer to facilitate the microstrip based feeds, since it is easy to have transitions from microstrip circuits to ridge waveguides. We can also directly excite the structure with waveguide feed arrangement and get rid off the ridge gap waveguide structure. It will be more cheap and compact, but it will only be compatible with waveguide feeds, whereas ridge gap waveguide interface can provide freedom of excitation means.

Fig.6.8 describes the return loss performance comparison with original pin period and modified pin period. Another modification in terms of the septum plate geometry has been introduced, which has particularly highlighted the trade-off between the circular polarization performance and the return loss performance, which will be discussed in the following sections as well.

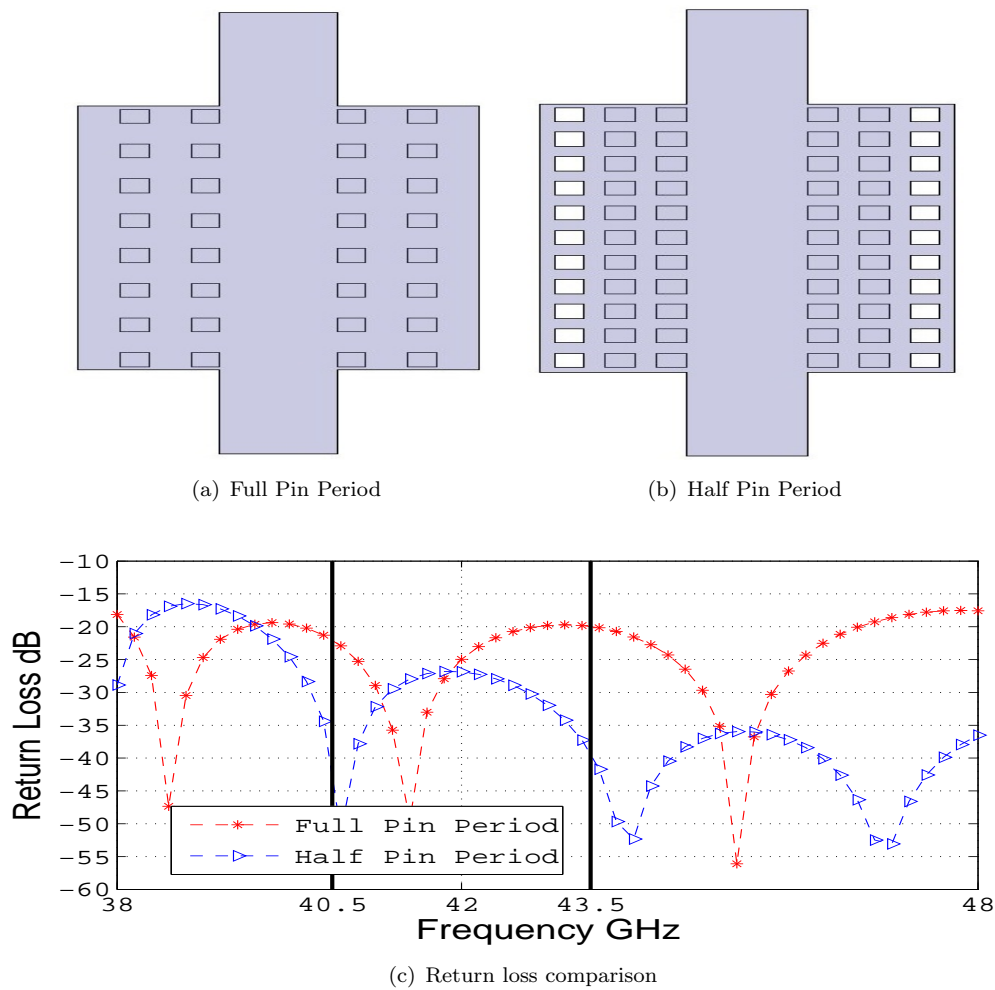


FIGURE 6.8: Return loss performance comparison for full and half pin period for GGWG

### 6.3.2.1 Single Layer Pin Texture

Recalling the gap waveguide concept from *chapter 3*, it was proposed to design the gap waveguide in three pieces, namely the top half, the lower half and the septum plate in between. This technique has been facilitated with pin texture only in the bottom half of the structure, that is why it has been termed as *Single Layer Pin Texture*. This technique however is not completely fulfilling the gap waveguide concept as the upper half still needs electrical contact between the side walls and the septum plate, this requires complex fabrication with more screws to avoid any leakage.

This technique however, has resulted in excellent circular polarization performance, even better than the existing standard waveguide based alternatives. Fig.6.9(c) shows the circular polarization performance comparison between the initially designed septum polarizer in standard waveguide technology and the gap waveguide based septum polarizer. The return loss performance has also shown in Fig.6.9(a) which is very reasonable.

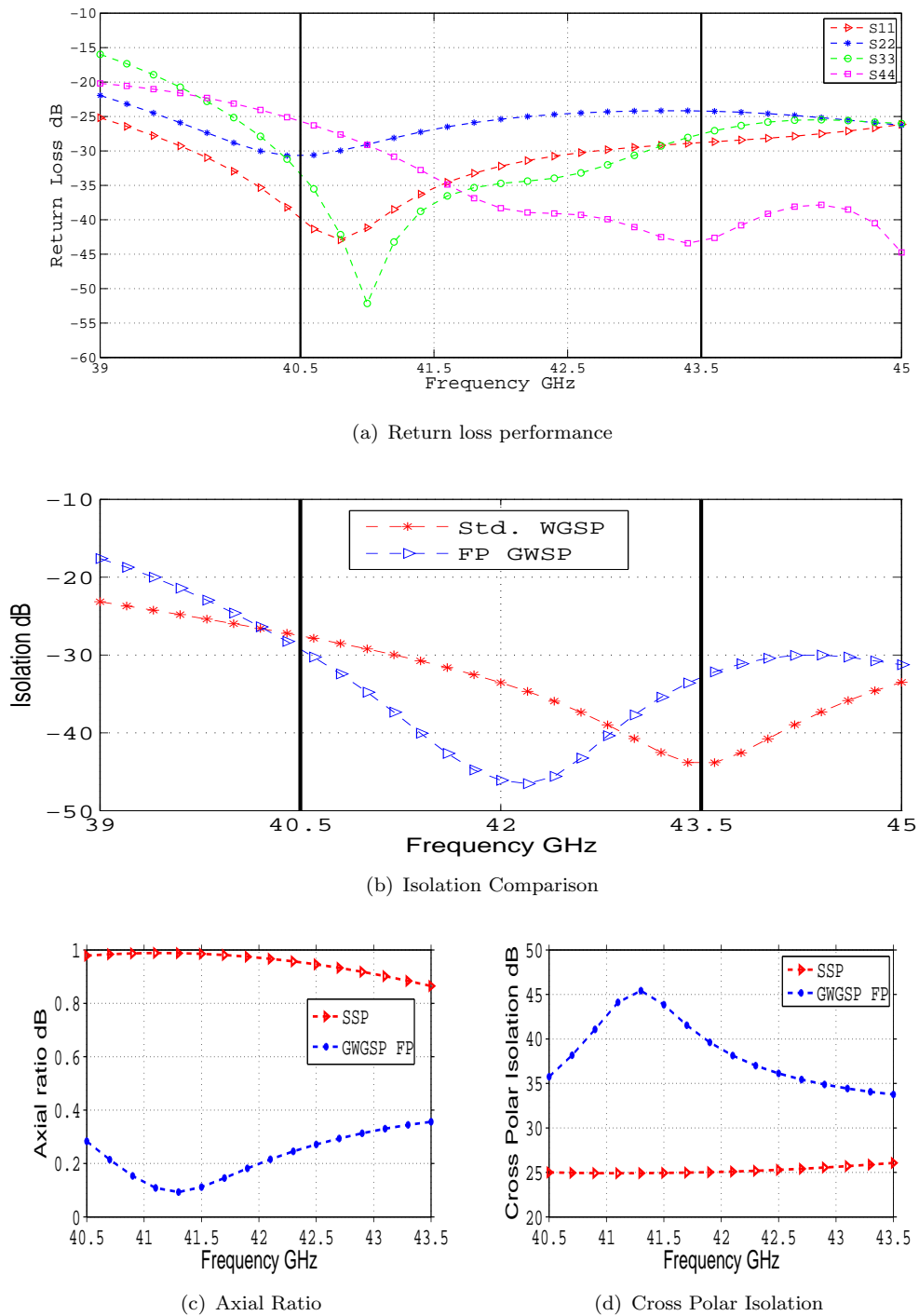


FIGURE 6.9: Return loss and circular polarization performance analysis for full plate GWGSP

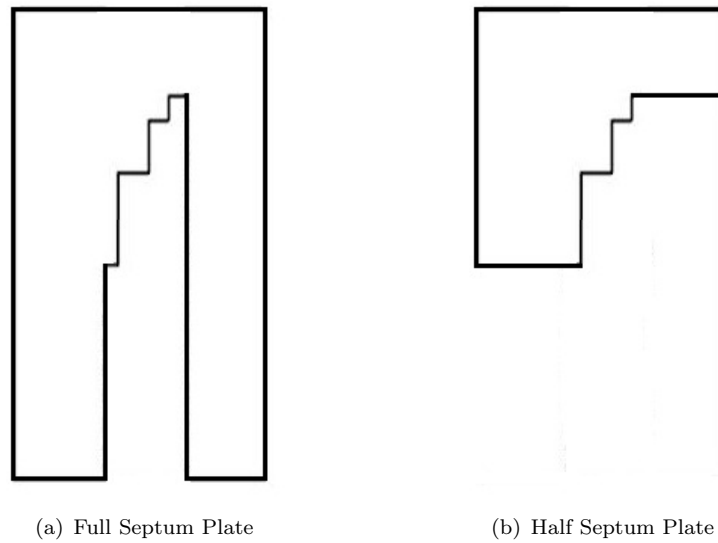


FIGURE 6.10: Full plate and half plate(truncated) septum geometry

As it has been mentioned earlier that there is always a trade off between the circular polarization performance and return loss performance, therefore attempts have been made to improve the return loss performance even further and these investigations have resulted in the classification of the design of the septum plate. A *full plate* refers to Fig.6.10(a) whereas a *half plate* refers to Fig.6.10(b). The full plate goes all the way between the upper and the lower halves whereas the half plate septum only extends in the transverse direction from the start and end of the septum steps as shown in Fig.6.10. The trade off between the circular polarization quality and device overall return loss performance can be estimated from Fig.6.9. A 3 dB improvement in return loss can be observed in Fig.6.11 when half plate septum was introduced. As a trade off 0.6 dB decrease in axial ratio can be seen in Fig.6.12 when half plate septum was considered.

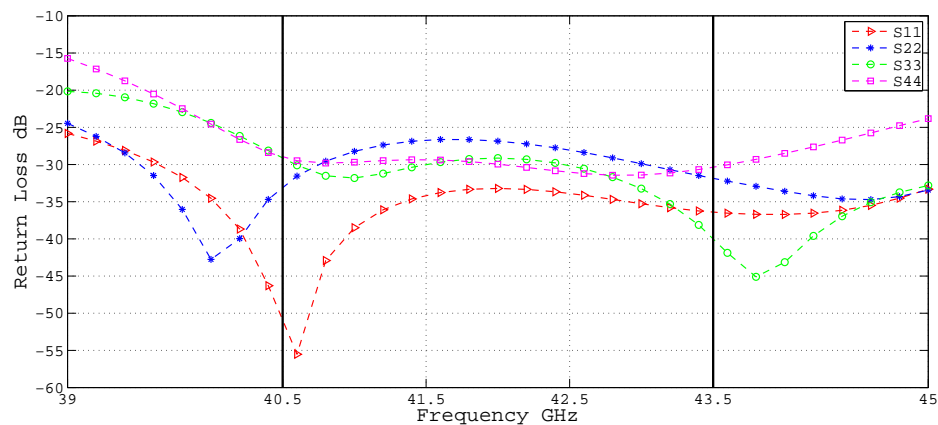
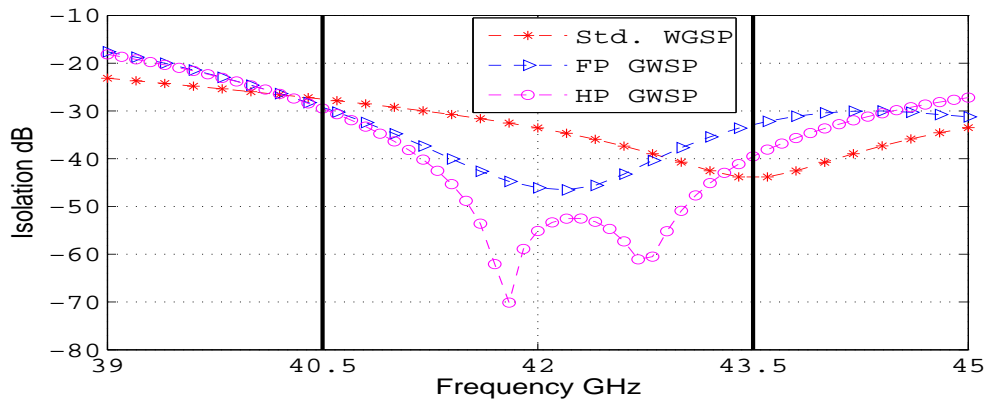
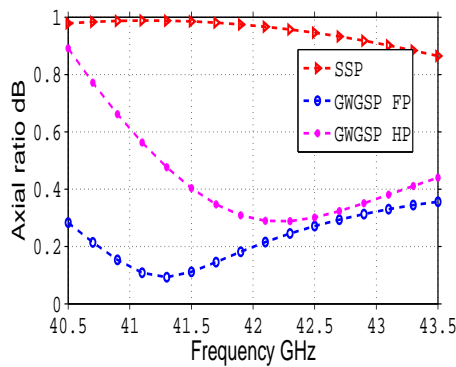


FIGURE 6.11: Return loss for septum polarizer with half plate

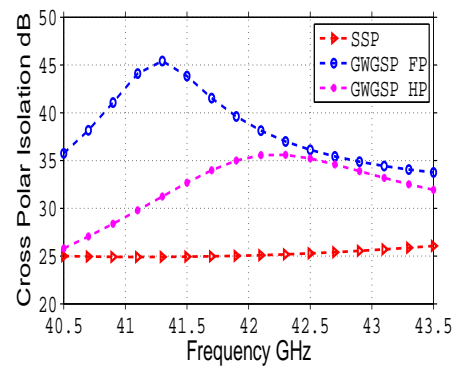
Fig.6.12 has presented a complete analysis. It is obvious that half plate septum has offered the best isolation performance, which is almost 40 dB down for majority of the



(a) Isolation comparison



(b) Axial Ratio



(c) Cross Polar Isolation

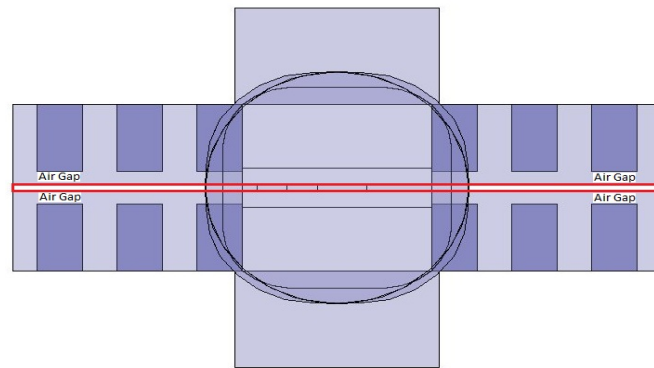
FIGURE 6.12: Circular polarization and isolation comparison

required frequency band. The return loss performance is almost same for all the three cases, however full plate septum has yielded the best circular polarization performance, which is almost  $0.3\text{dB}$  down for the complete frequency band.

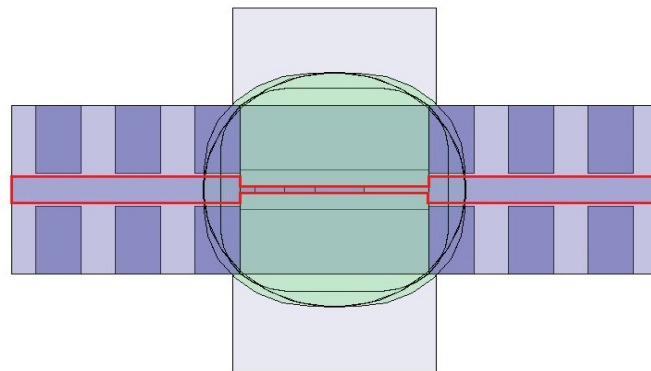
*Concluding the whole analysis, we can surely state that gap waveguide based septum polarizers with either implementation i.e full plate or half plate, are very good in overall performance as compared to the existing standard waveguide based alternatives, which has motivated the need to explore more into the gap waveguides.*

### 6.3.2.2 Double Layer Pin Texture

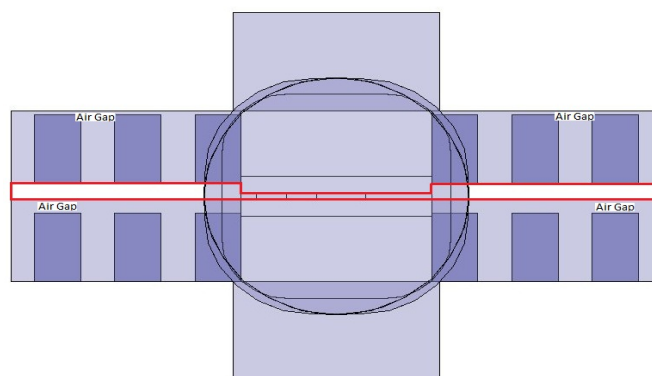
The term *Double Layer Pin Texture* refers to introducing metal pins on both halves (upper and lower) to the septum plate, to implement the gap waveguide concept fully when septum polarizers are required to design in this technology. It has been discussed above that the single layer pin texture does not fulfil the gap waveguide requirement completely since the upper half still requires electrical contact for the side walls, so this section concludes the performance of the OMT when pins were introduced to the upper half as well. Again various approaches have been analysed.



(a) Model 1

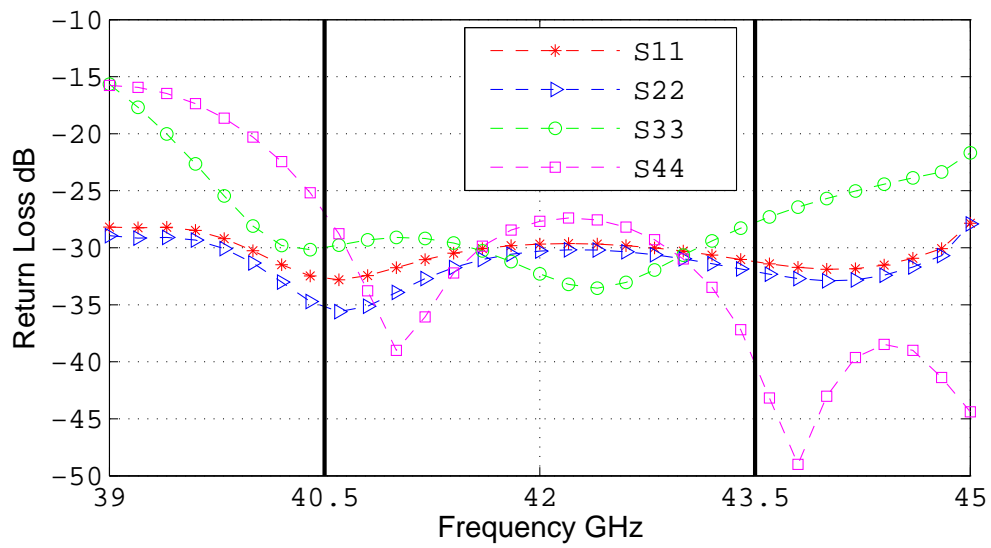


(b) Model 2

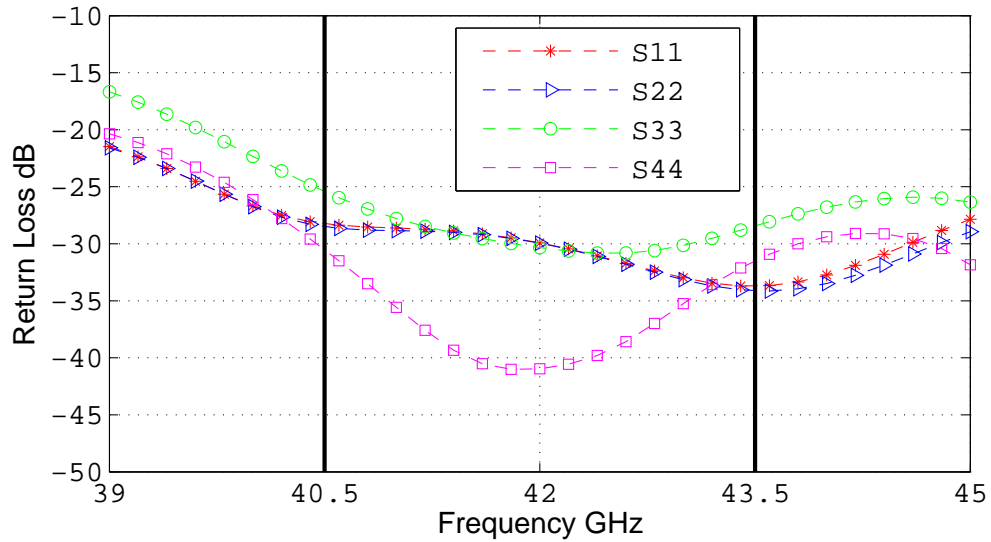


(c) Model 3

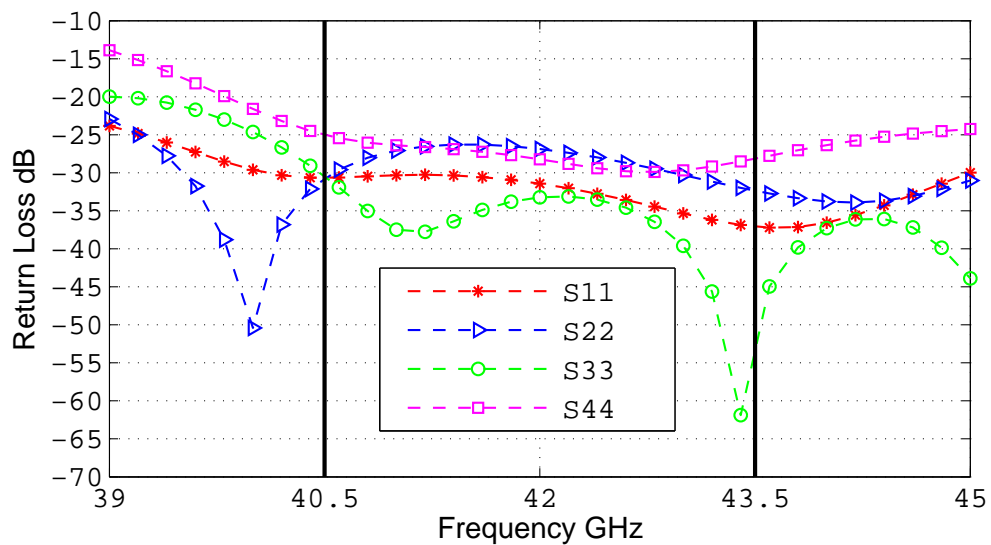
FIGURE 6.13: Front view of double layer pin texture based septum polarizer. Red bounded region defines the septum plate geometry



(a) Model 1



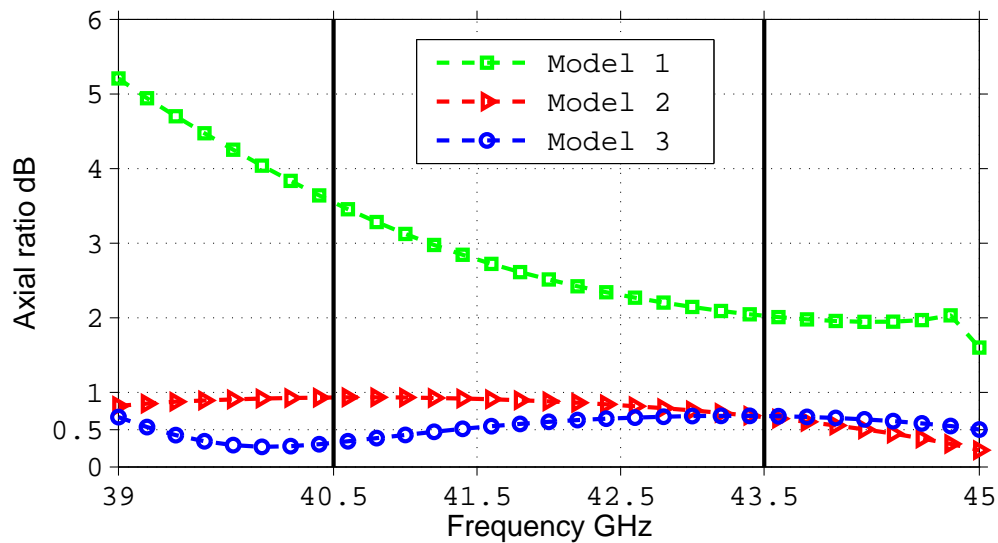
(b) Model 2



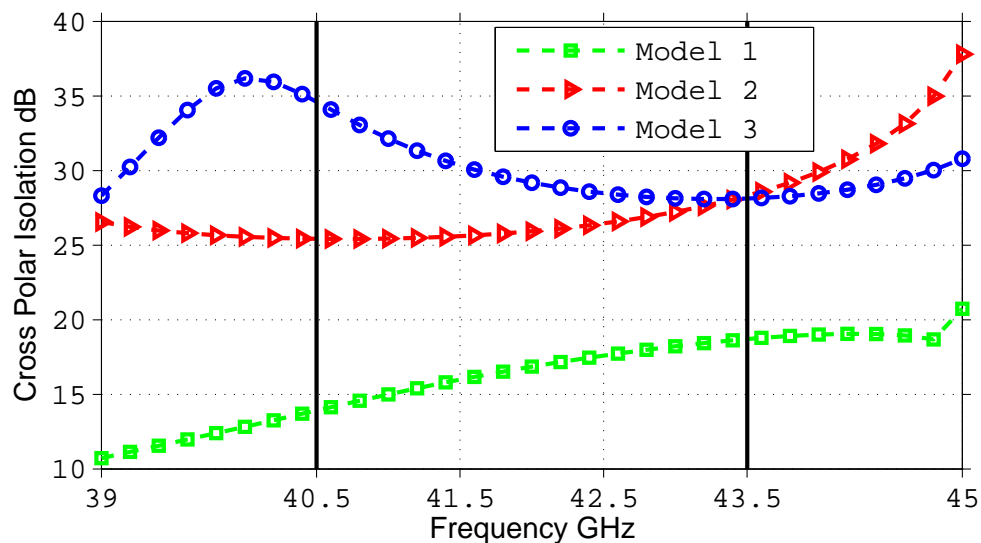
(c) Model 3

FIGURE 6.14: Return loss performance of various double pin textured models

The double layer pin texture has been simulated using three different techniques, as described by Fig.6.13. Model 1 is symmetrical in nature and it offers very good return loss performance as shown in Fig.6.14(a), however it has resulted in very poor circular polarization performance described by Fig.6.15(b). It seemed that the  $TE_{01}$  mode was not compatible with the double pin septum approach with a bit wide air gap in between, which might be the cause for poor axial ratio i.e 3.6 dB. Model 2 of Fig.6.13(b) presents a modified version of the septum, since it was required to reduce the air gap to improve the circular polarization performance.



(a) Axial Ratio Comparison



(b) Cross Polar Isolation Comparison

FIGURE 6.15: Front view of double layer pin texture based septum polarizer. Red bounded region defines the septum plate geometry

The septum was made thick from the edges as shown by red line in Fig.6.13(b). The

return loss performance did not change very much and is still acceptable however a major increase in circular polarization performance can be observed from Fig.6.15(b). While varying the septum geometry to improve the axial ratio even further, I have finalized the septum geometry described by Fig.6.13(c), since it offers the same return loss performance with a much better circular polarization performance as well. An axial ratio of approximately  $0.6dB$  was achieved with a cross polar isolation better than  $30dB$  as shown in Fig.6.15(a).

The double pin texture approach has resulted in much better over all device performance, but it is still not better than what we have achieved from single layer pin texture approach discussed in previous section. Furthermore these results have been obtained on the cost of very small air gap of  $0.1mm$  between the pins and top plate which might not be realizable, but it is still subjected to the accuracy of milling machines, which varies from company to company.

## 6.4 Quarter Wave Plate

Quarter wave plate is a device that introduced  $90^\circ$  phase delay to that component of the net electric field, which is propagating parallel to the plate. Since an ideally circularly polarized signal has two orthogonal components, therefore introducing  $90^\circ$  phase delay to one of the components will result in linear polarization and vice versa. The quarter wave plate has been designed in a standard quadratic waveguide and is composed of Teflon with relative permittivity ( $\epsilon_r = 2.2$ ).

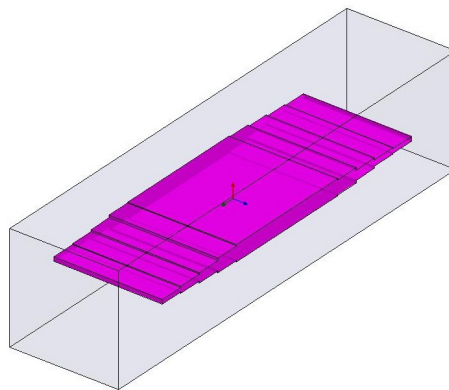


FIGURE 6.16: 3D view of the quarter wave plate

The dielectric slab has been designed in steps to provide maximum matching. Return loss better than  $25dB$  has been achieved, as described by Fig.6.17. The return loss performance of Fig.6.17 is sufficient since improving further will make it hard to realize the dielectric plate. The addition of this quarter wave plate has resulted in linear polarization in  $45^\circ$  plane, therefore the whole structure can be rotated  $45^\circ$  and the OMT

can be interfaced with the feed horn using 2 step quadratic to circular transition, that has been described in later section.

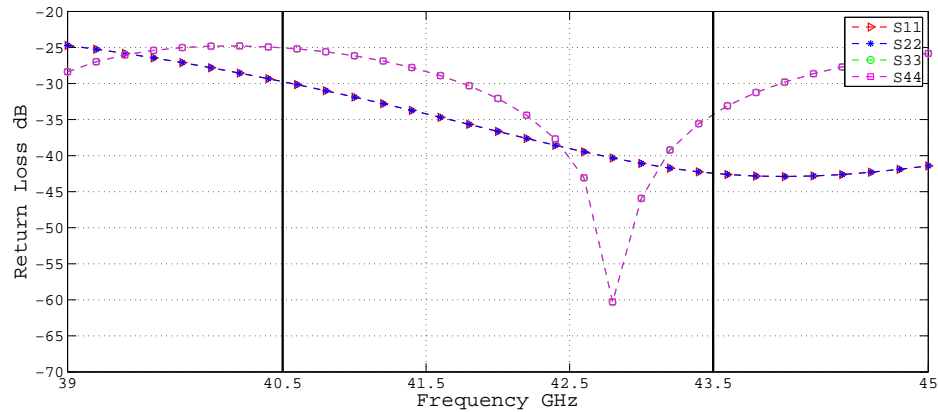


FIGURE 6.17: Return loss performance for the quarter wave plate

## 6.5 Right Angle E Bend

Since the design of septum polarizers usually do not end up in standard quadratic apertures, so a step transition is mostly required to interface the device with the standard excitation setup. A right angle E bend has been designed with R500 standard input flange. Fig.6.18 is showing its 3D and side view, however the return loss performance has been shown in Fig.6.19. The structure has offered a return loss better than  $39dB$  over the desired frequency band.

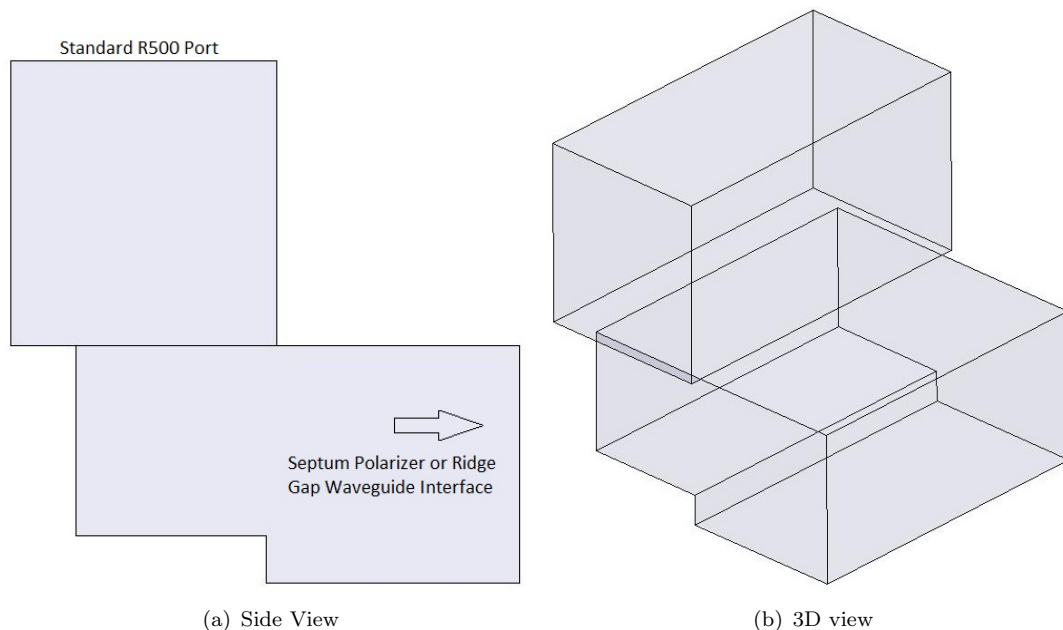


FIGURE 6.18: Geometrical view of the right angle E bend

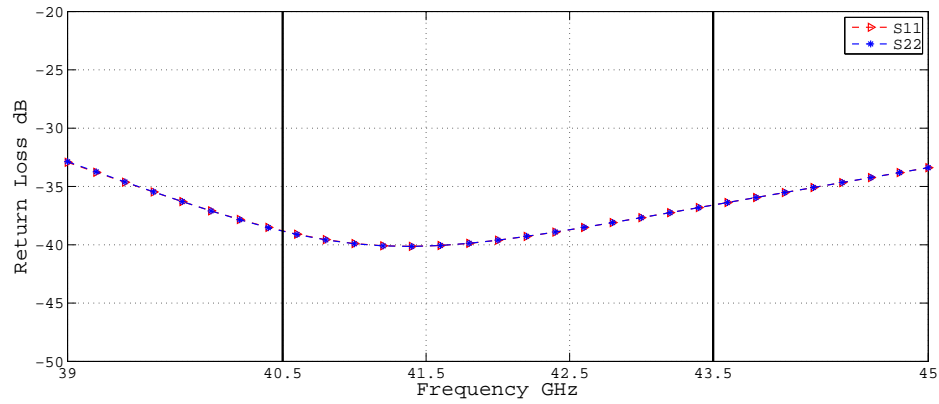


FIGURE 6.19: Return loss performance for the right angle E bend

The E bend has been designed in a step like fashion instead of the mitered edge, because it is more wideband and easy to mill structure. The bandwidth of operation can be increased by introducing a few more steps, but in our case, only a single step has fulfilled our return loss and bandwidth requirements.

## 6.6 Quadratic to Circular Transition

A two step quadratic to circular transitions has been designed for the fact that the quadratic aperture at the output of the septum polarizer was not compatible with the standard excitation setup, and furthermore the quarter wave plate provides linear polarization in  $45^\circ$  plane, so by the aid of this transition the OMT can be rotated  $45^\circ$  to excite the feed horn with the right linear polarization. The geometrical view of the transition has been shown in Fig.6.20.

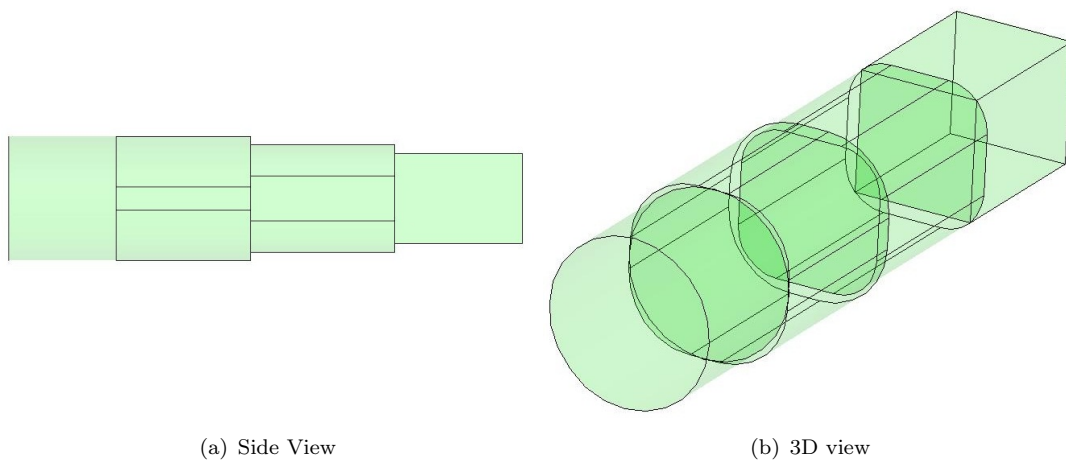


FIGURE 6.20: Geometrical view of the quadratic to circular transition

The return loss from Fig.6.21 was found to be better than  $40\text{ dB}$  for the desired frequency band. Two step transition was more than enough for almost 10 percent bandwidth. More

steps may be added for wider frequency bands, but they will off course make the overall structure large in length.

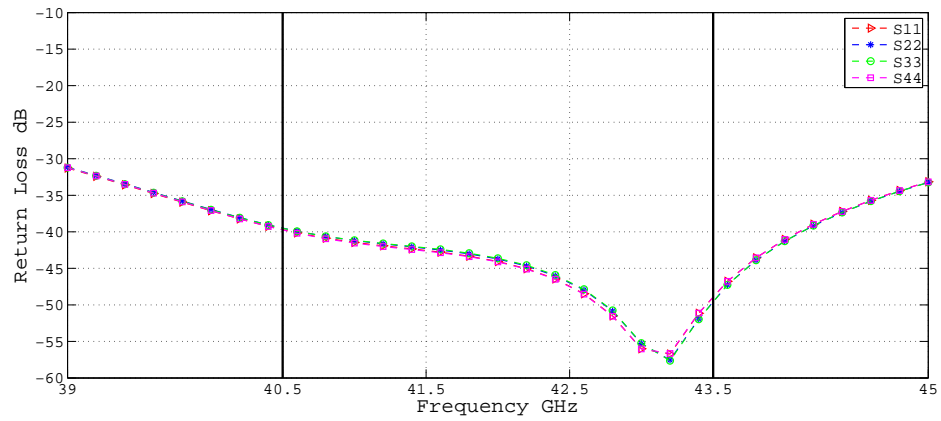


FIGURE 6.21: Return loss performance for the quadratic to circular transition

## Chapter 7

# Prototype Design

We have established in the previous chapter that gap waveguide based septum polarizer has proved to be much better than the existing standard waveguide based alternatives, in terms of return loss, isolation and circular polarization performance. It was also discussed that a ridge gap waveguide might be interfaced with the septum polarizer to facilitate microstrip based feed networks. However if a waveguide feed setup is available, there is no need to include the ridge gap waveguide structure, which will merely increase the overall structure length. Arkivator telecom has shown interest in the *Single Layer Textured Septum Polarizer* discussed in *section 6.3*, since it offers excellent circular polarization performance with very good return loss performance as well. The geometrical views of the structure are shown in Fig.7.1.

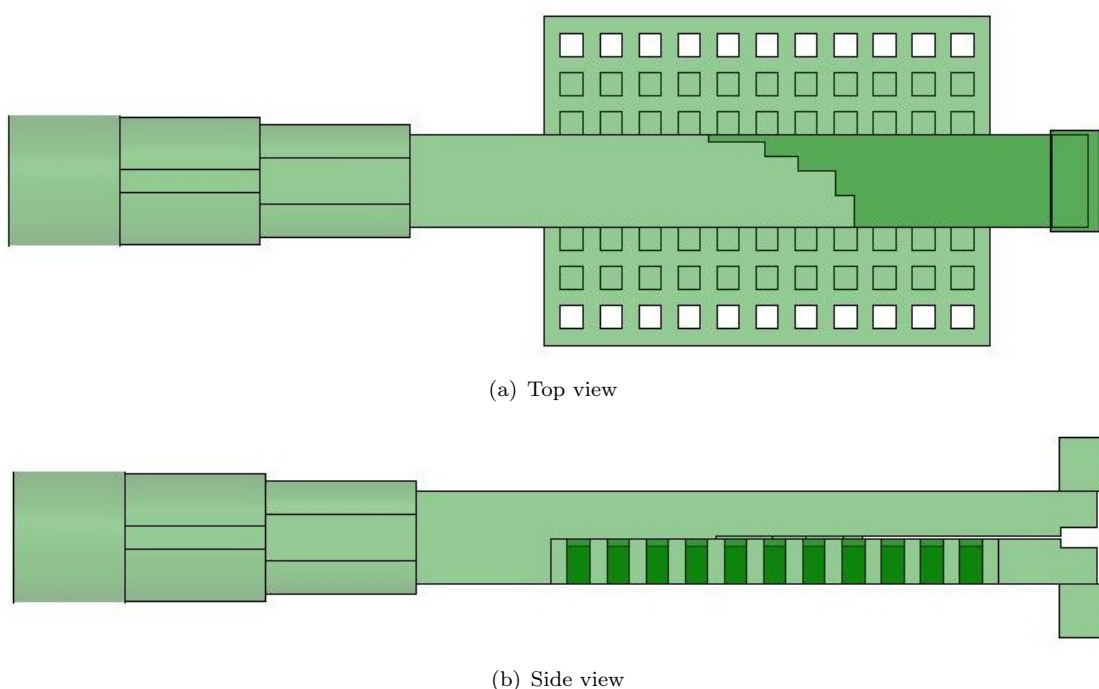


FIGURE 7.1: GWGSP Prototype Geometry

## 7.1 Simulated Results

The simulations have been done in HFSS and the results have been discussed in the previous chapter. These results are presented here just as a refresher for the reader to highlight the performance comparison.

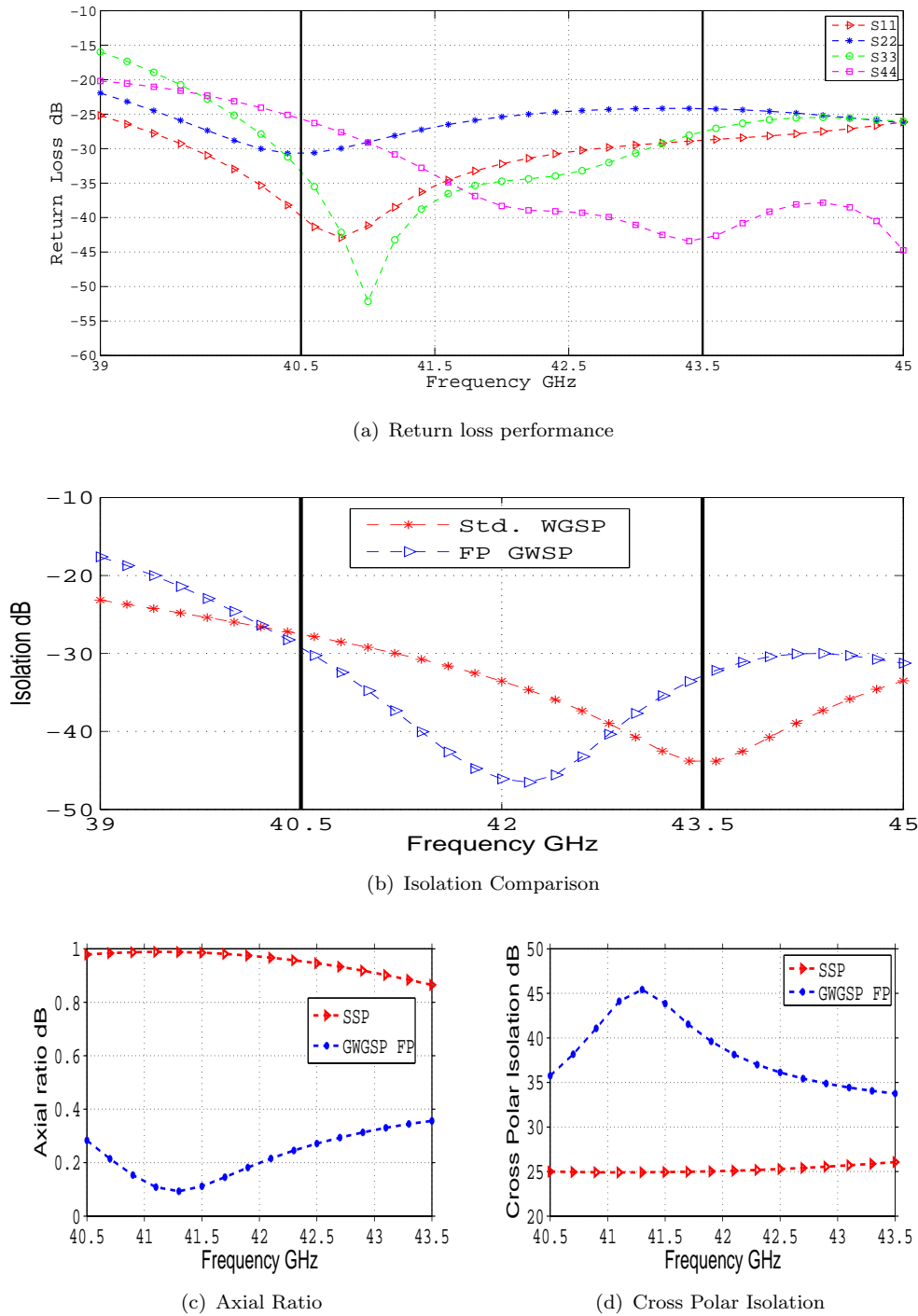


FIGURE 7.2: Return loss and circular polarization performance analysis for full plate GWGSP

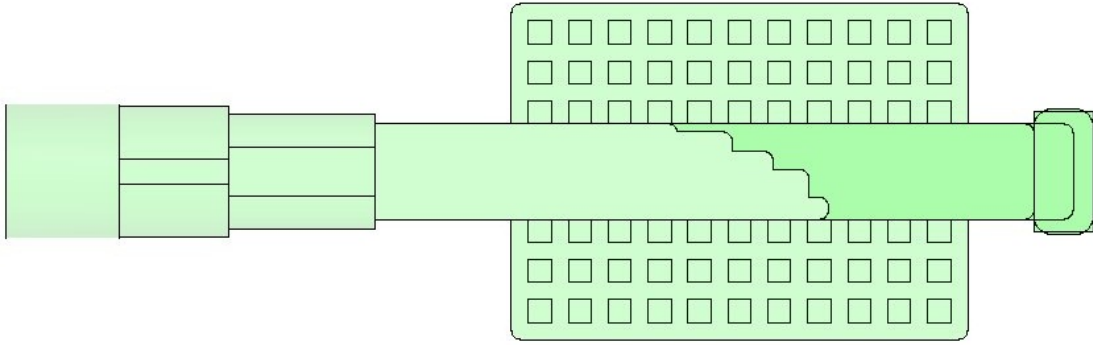


FIGURE 7.3: CAD based modified geometry

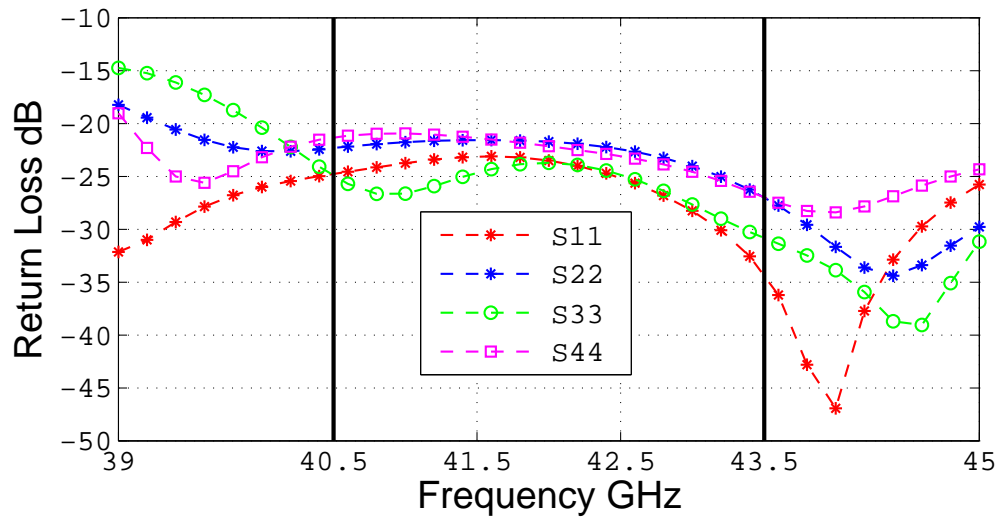
It has been established that the gap waveguide based septum polarizer has better performance than existing standard waveguide based alternatives. This can be reviewed from Fig.7.2.

## 7.2 Prototype CAD Analysis

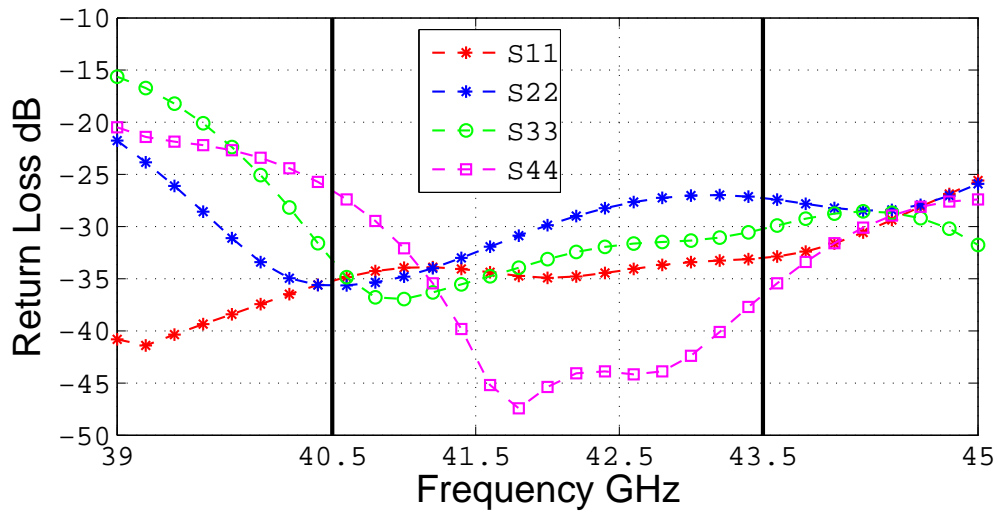
The design of Fig.7.1 has been submitted for fabrication. We know that manufacturing process introduces tolerances in the dimensions depending upon the sensitivity of the milling machines. Usually these tolerances are not known a priori, therefore depending upon the amount of tolerances introduced, the electrical performance of the device may vary. The CAD based modified design from Arkivator's workshop has been shown in Fig.7.3.

It can be observed that the septum and the input ports have been introduced with radii, which has degraded the device performance. The return loss in Fig.7.4(a) has increased by almost 5 to 8dB which has also degraded the axial ratio performance of the device. The design has been reoptimized for the best performance with the available machining limitations. Fig.7.4(b) describes the optimized return loss performance for the geometry in Fig.7.3. It can be seen that the re-optimization has improved the return loss performance which is almost identical to the initially submitted design.

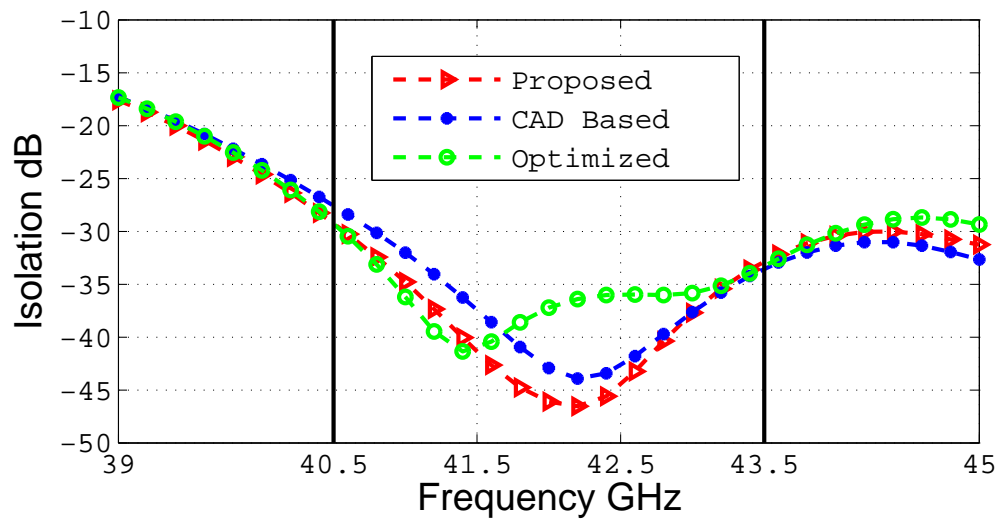
The isolation and circular polarization performance comparisons for the proposed (initially submitted Fig.7.1(a)), CAD modified (workshop modified Fig.7.3) and finally optimized structures have been presented in Fig.7.5. It can be observed that the isolation performance remains almost the same for all three versions, however the axial ratio performance has improved a lot. It is almost 0.2 dB and below for half of the desired frequency band. At lower frequency edge, it is a bit raised but still acceptable. Attempts have been made to improve it for the lower frequency edge as well, but it resulted in an increase in return loss performance.



(a) CAD based modified structure



(b) Optimized structure



(c) Isolation comparison

FIGURE 7.4: Return loss and isolation performance for CAD modified and re-optimized structures

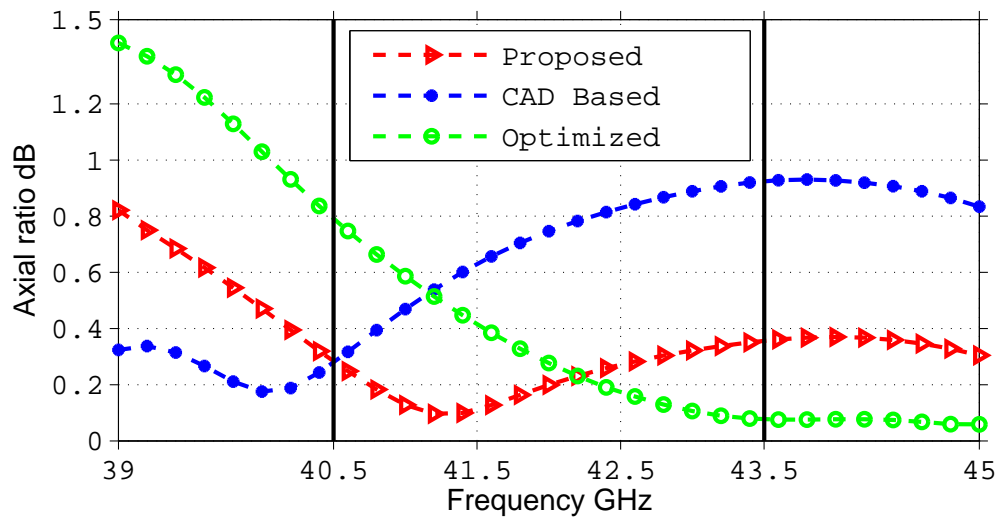


FIGURE 7.5: Axial ratio performance analysis for proposed, modified and re-optimized structures

### 7.3 Downscaled Structure Analysis

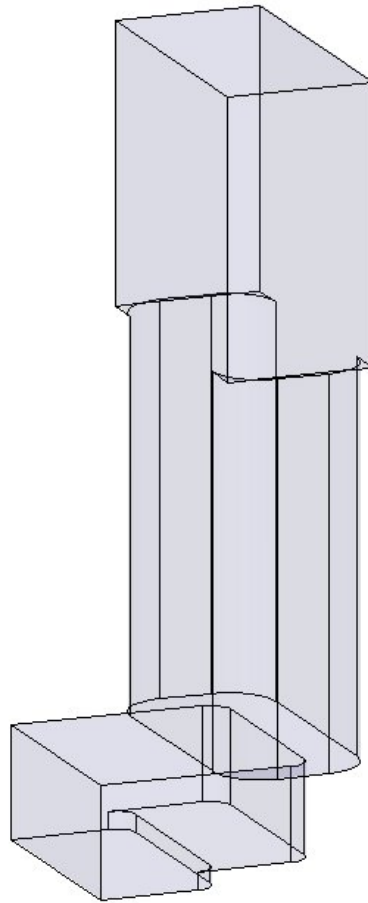
[h!] It has been shown in the previous section that re-optimizing the structure as per fabrication limitations has resulted in fairly well electrical characteristics. The re-optimized design can be placed forward for fabrication but it has been downscaled to operate in Ku band, merely for measuring puposes. The downscaled structure operated well for almost 10 percent bandwidth centered at 15 GHz. The equipment at Chalmers Antenna Group facilitates the device measurements for almost 20 GHz and below. In principle, downscaling the strucutre must yield the same electrical performance, however every component cannot be exactly downscaled due to the fact that the input and output ports must follow standard waveguide dimensions.

#### 7.3.1 Input E bend optimization

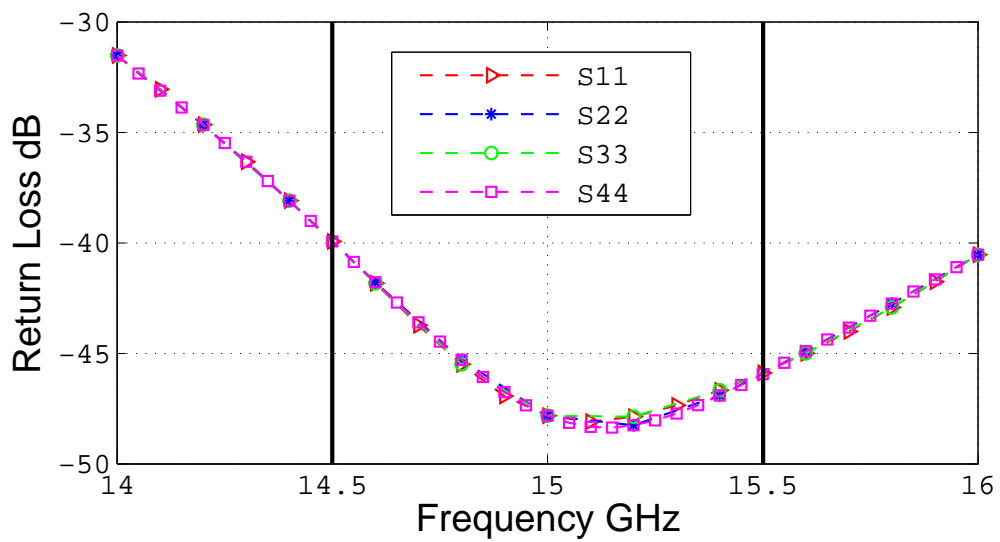
The input E bend and the circular output ports have been omptimized separately, with the radius compensations effects included. The same structure with a little bit of tuning has resulted in the desired electrical performance. The return loss in Fig.7.6(b) has made better than 40dB for almost 10 percent bandwidth centered at 15 GHz.

#### 7.3.2 Quadratic to Circular Transition optimization

As described in earlier sections that a quadratic to circular transition was designed to interface the OMT with the feed horn. The re-optimized downscaled version has resulted in a very good electrical performance as described in Fig.7.7.

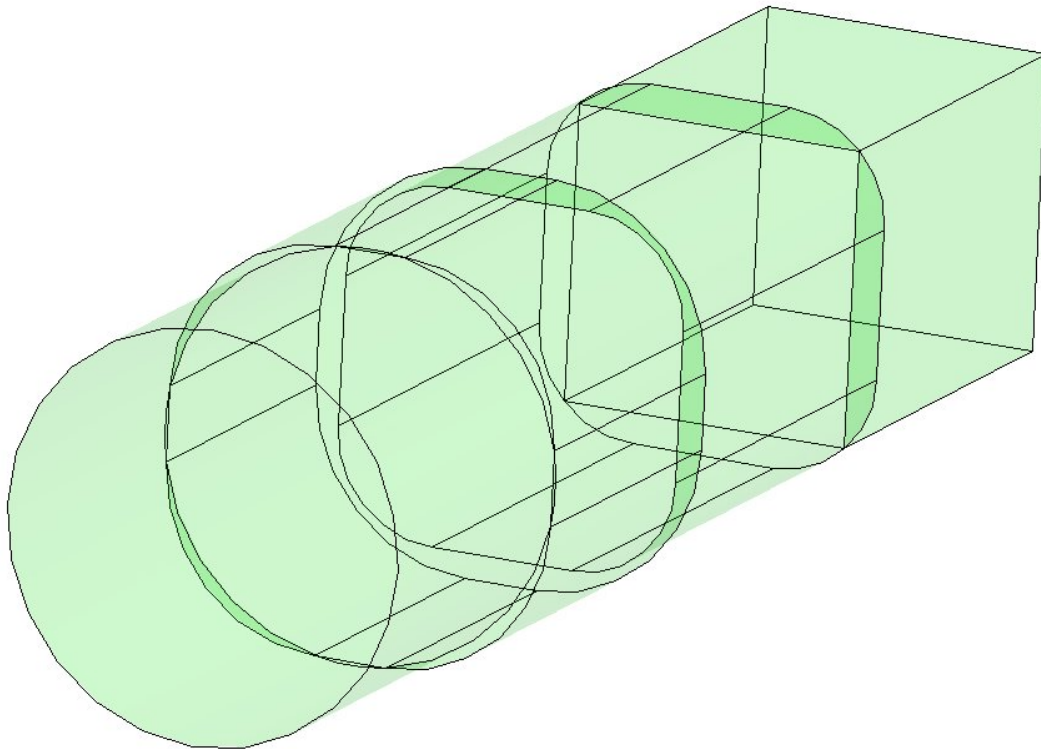


(a) E bend 3D view

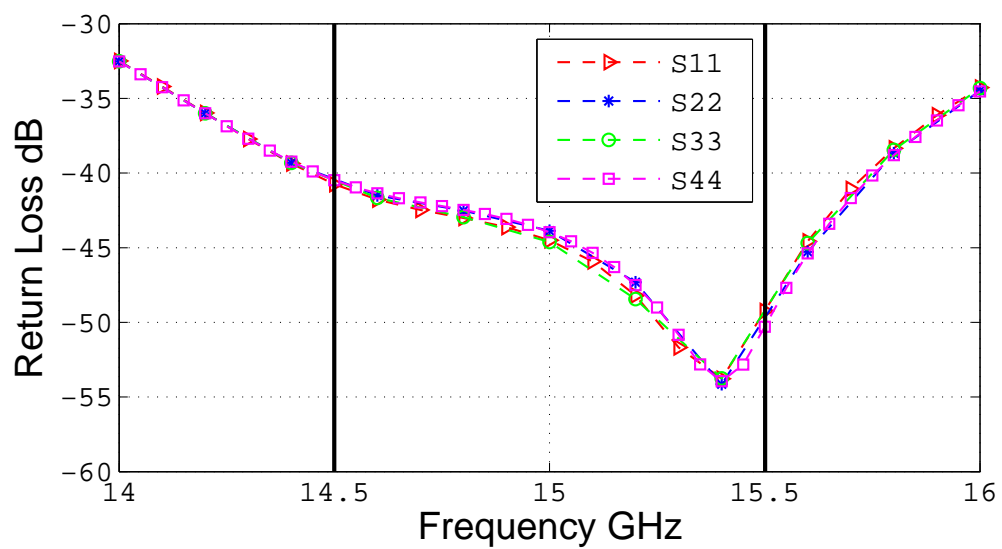


(b) Return loss performance

FIGURE 7.6: 3D view and return loss performance of downscaled E bend



(a) Quadratic to circular transition 3D view



(b) Return loss performance

FIGURE 7.7: 3D view and return loss performance of downscaled QST

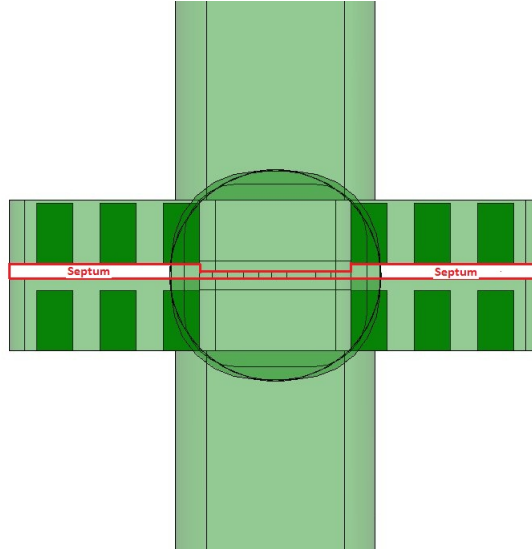


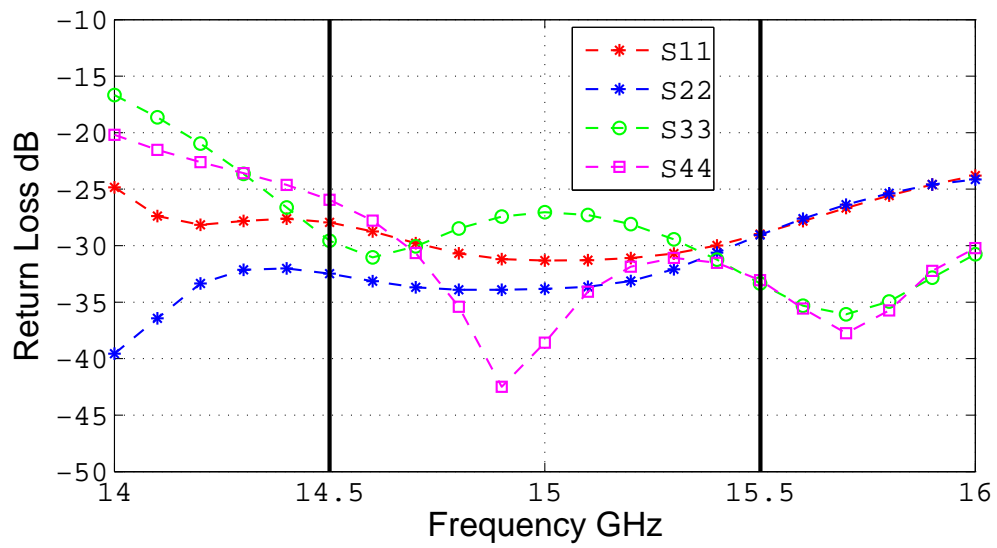
FIGURE 7.8: Cross sectional view of the double layer pin structure

## 7.4 Optimized Double Layer Pin Structure

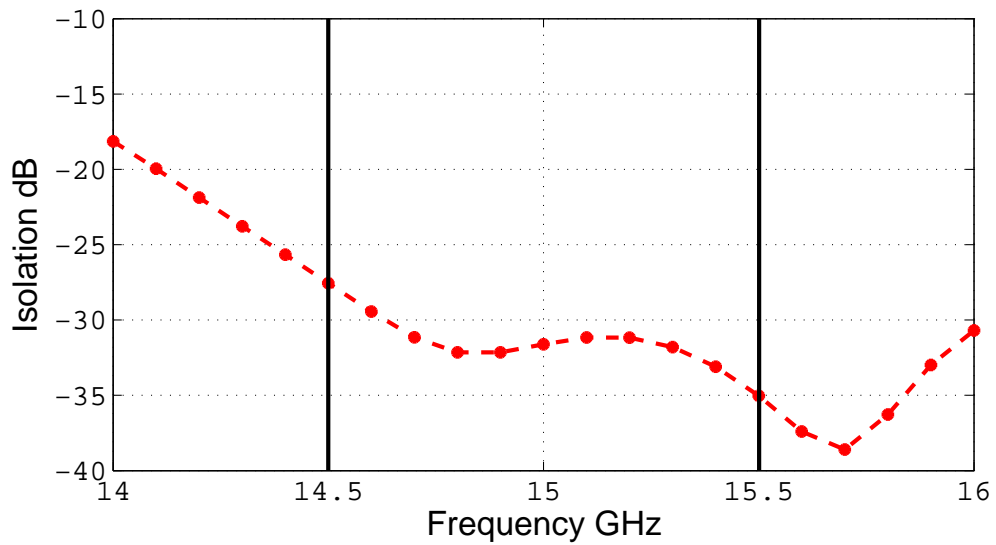
In the previous chapter, we have presented in detail about the single layer and double layer pin structures. The double layer pin structure fulfills the gap waveguide condition in a complete sense, however it is a fact that the gap height  $h$  is a critical factor that effects the electrical as well as circular polarization performance of the structure. Down-scaling the structure has provided means to physically realize the gap height, which was considered to be critical for the high frequency designs, since the gap heights become very small with increase in operating frequency.

A cross sectional view of the double layer pin structure has been shown in Fig.7.8, followed by its return loss, isolation and circular polarization performance in Fig.7.9. It can be observed from Fig.7.8 that the septum geometry is not usual and non symmetric, even the gap height for the upper layer of pins is not identical to the lower half. Several combinations have been investigated to optimized for the best performance, and this approach has resulted in a reasonable agreement. Decreasing the gap height can even further improve the device performance but it will not be physically realizeable any more.

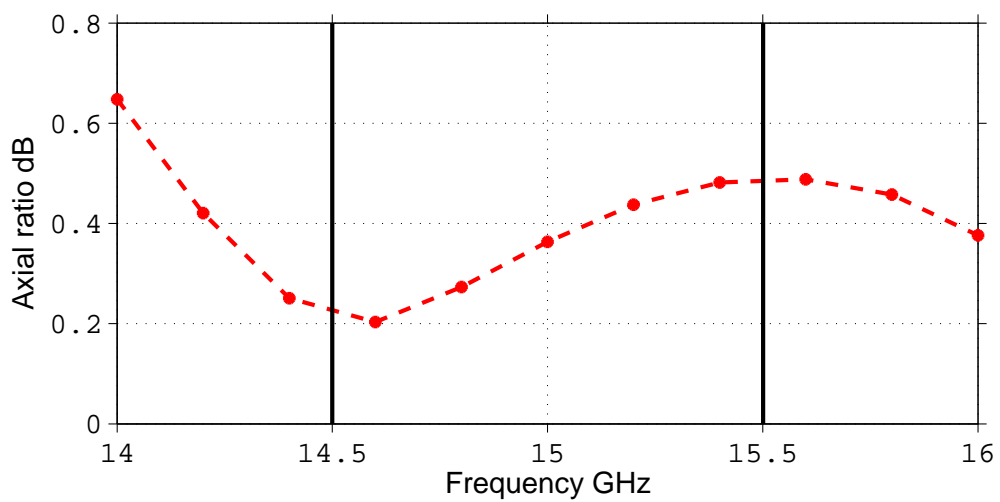
The return loss is very reasonable as it is better than 27dB, however the isolation performance is almost better than 30dB. The isolation can be improved by modifying the septum thickness, however return loss and circular polarization performance is dependent upon the pin arrangement in the upper half, as we can refer to the discussion in the previous chapter. The axial ratio performance is however very reasonable.



(a) Return Loss



(b) Isolation

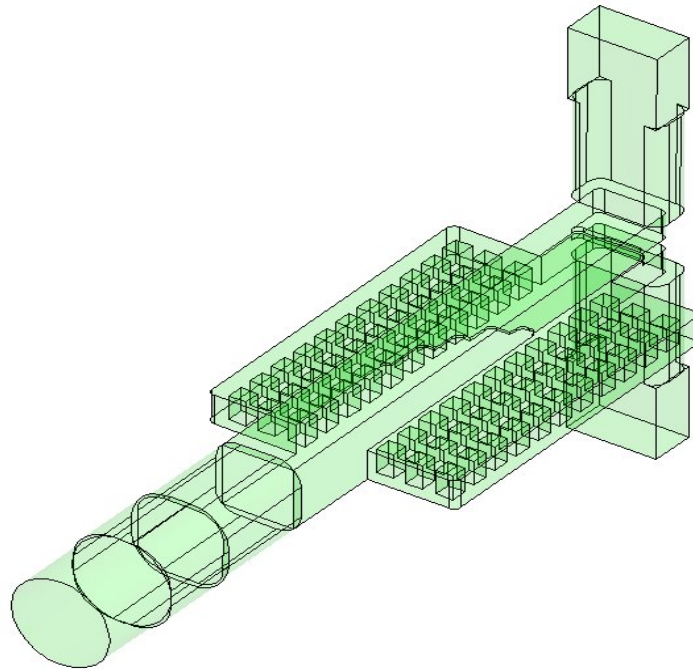


(c) Axial Ratio

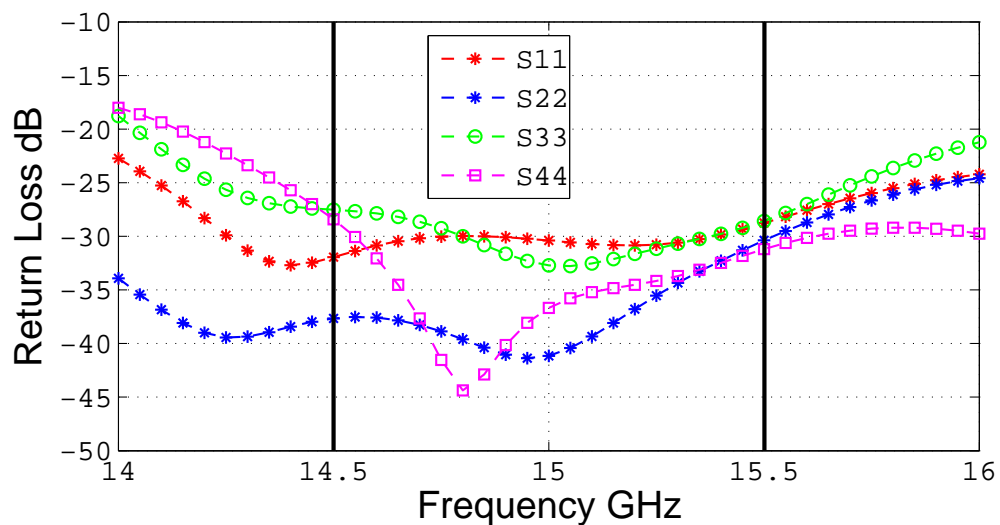
FIGURE 7.9: Electrical performance for double layer pin texture

## 7.5 Optimized Single Layer Pin Prototype Model

The individual downscaled and re-optimized components are interfaced together to produce the desired OMT structure, that operates on Ku band. The 3D view has been shown in Fig.7.10(a).

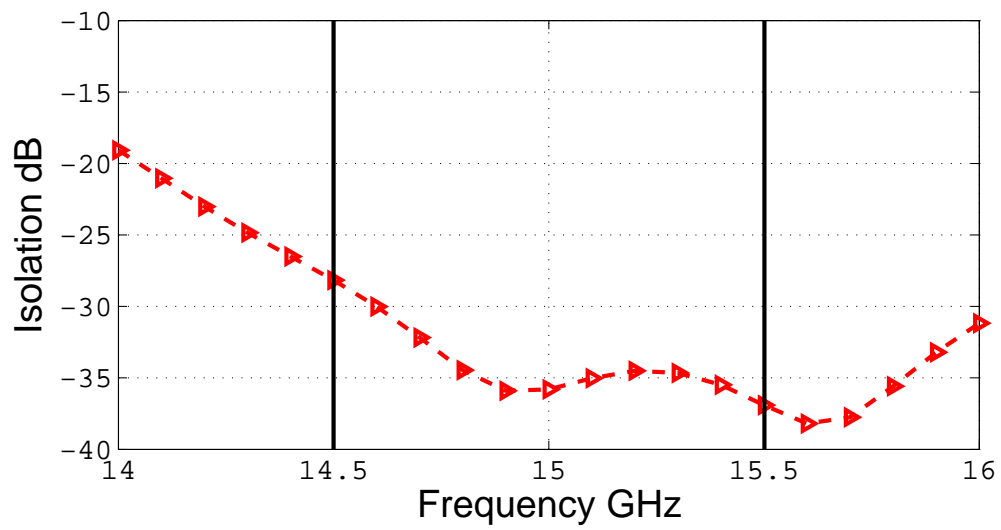


(a) 3D view of the optimized prototype model

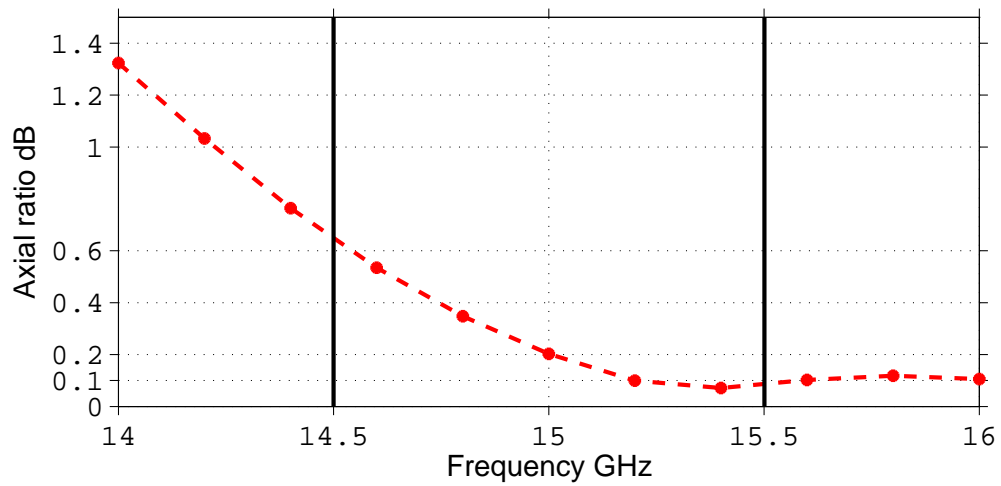


(b) Return loss performance

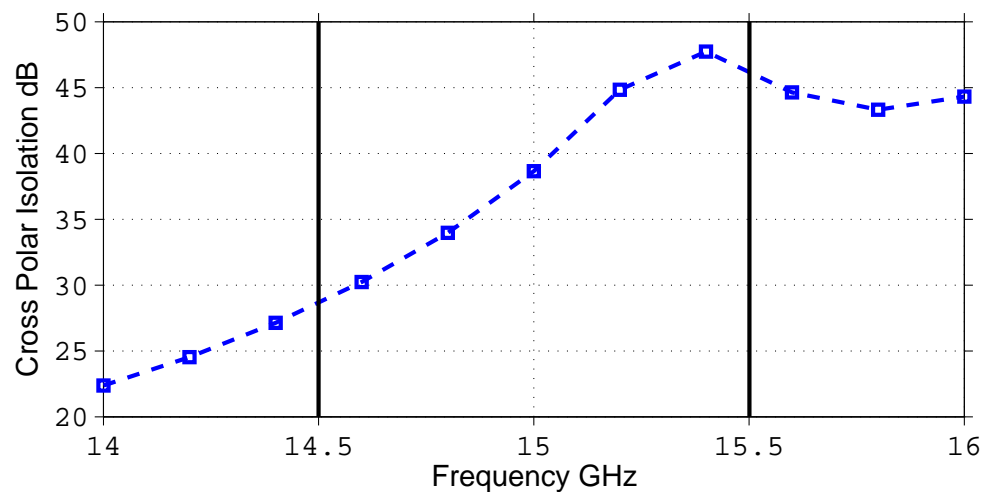
FIGURE 7.10: 3D view and return loss performance of downscaled prototype model



(a) Isolation Performance



(b) Axial Ratio



(c) Cross Polar Isolation

FIGURE 7.11: Isolation and circular polarization performance

The return loss in Fig.7.10(b) has even improved further upto a level of 30dB and better for the desired frequency band. The isolation in Fig.7.11(a) however remains the same, which can be improved by modifying the septum thickness and dimensions, but this may degrade the axial ratio performance. The axial ratio in Fig.7.11(b) is almost 0.1 dB and below for majority of the frequency band along with with good cross polar isolation level.

The downscaled single layer pin model has been submitted for fabrication, which will be measured afterwards. A close agreement between the simulated and the measured results is expected, since the simulated results have included the manufacturing tolerances. The measured results will be updated in the following version of this thesis report.

# Conclusion

This report has demonstrated the design of an orthomode transducer in the recently introduced gap waveguide technology. Various approaches for the implementation of gap waveguide concept have been implemented and discussed in detail. The initial design was composed of a ridge gap waveguide interfaced with the septum polarizer followed by a quarterwave plate to operate with linear polarizations. However the final design is very compact and is compatible for circular polarization only. In fact the OMT was required to operate for 40.5 to 43.5 GHz band, but the design placed for manufacturing, operates at Ku band. The later is a downscaled version of the high frequency design, which means that a successful design for the high frequency band has been presented as well. In fact the design at Ku band is compatible with the measuring facilities available at the antenna group, Chalmers University of Technology. The downscaled version has been extensively optimized to work for almost 10 percent bandwidth centered at 15 GHz, maintaining a return loss better than 30dB with an isolation better than 35dB for the band of interest. This gap waveguide based OMT has produced excellent circular polarization quality, i.e. an axial ratio better than 0.2dB with a cross polar isolation better than 40dB for most of the desired frequency band, which is even better than the existing standard waveguide based alternatives.

Due to the timeline limitations and some delays in the fabrication process, the measured results could not be included in this report, however based on previous experience with HFSS we would expect quite close agreement between the measured and simulated results. The measurements will be done in a few weeks by the PhD students in the antenna group, and if the results are as expected we will submit the work to the EuCAP2010 conference to be held in Rome in July 2011.

The design needs further investigations in order to completely implement the gap waveguide concept, since the single layer pin structure still requires very good electrical contact in the upper half of the overall structure. Although this has been facilitated by fabricating the septum as a part of the upper half waveguide, but still it requires a few more screws to avoid leakage. Alternatively a double layer pin texture is also designed and thoroughly presented, which has fulfilled the complete gap waveguide condition, however it has been observed that this design needs careful investigation at higher frequency bands, since physical realization of a very narrow gap height is very critical.

# Bibliography

- [1] A. Valero-Nogueira E. Rajo-Iglesias P.-S. Kildal, E. Alfonso. Local metamaterial-based waveguides in gaps between parallel metal plates. *IEEE Antennas and Wireless Propagation letters (AWPL)*, Vol.8:84–87, Year 2009.
- [2] Eva Rajo. Per-Simon Kildal, Ashraf Uz Zaman. *submitted to IEEE transactions microwave theory and techniques*.
- [3] J. R. Costa M. G. Silveirinha, C. A. Fernandes. Electromagnetic characterization of textured surfaces formed by metallic pins. *IEEE Trans. Antennas Propagat.*, Vol. 56, No. 2:405–415, Feb. 2008.
- [4] P.-S. Kildal and A. Kishk. Em modelling of surfaces with stop or go characteristics-artificial magnetic conductors and soft and hard surfaces. *App. Comput. Electromagn. Soc. J.*, Vol.18,no.1:32–34, March 2003.
- [5] P.-S. Kildal. Three metamaterial-based gap waveguides between parallel metal plates for mm and submm waves. *3rd European Conference on Antennas and Propagation*, vol.:23–27, Year 2009.
- [6] Per-Simon Kildal. *Foundation of antennas, a unified approach*. Compendium in Antenna Engineering at Chalmers,2009, 2009.
- [7] Jens Bornemann Jarosla Uher. *Waveguide components for antenna feed systems: Theory and Cad*. Addison Wesley, 1976.
- [8] P.-S. Kildal. Definition of artificially soft and hard surfaces for electromagnetic waves. *Electron. Lett.*, Vol.24,no.3:168–170, Feb. 4 1988.
- [9] Romulo F. Jimenez Broas Nicholas G. Alexopolous Dan Sievenpiper, Lijun Zhang and Eli Yablonovitch. High-impedance electromagnetic surfaces with a forbidden frequency band. *IEEE transactions on Microwave Theory and Techniques*, Vol. 47, No. 11:1–2, November 1999.
- [10] P.-S. Kildal Eva. Rajo-Iglesias. Cut-off bandwidth of metamaterial-based parallel plate gap waveguide with one textured metal pin surface. *3rd European Conf. Antennas Propagat. (EuCAP 2009), Berlin, Germany*, Vol.:23–27, March 2009.

- 
- [11] L. Inclan E. Rajo-Iglesias, M. Caiazzo and P.S Kildal. Comparison of bandgaps of mushroom-type ebg surface, corrugated and strip-type soft surfaces. *IEEE transactions on Microwave Antennas Propagation*, Vol. 1, No. 1:1–2, Feb 2007.
- [12] Ashraf Uz Zaman E. Rajo-Iglesias and P.S Kildal. Parellel plate cavity mode suppression in microstrip circuit packages using a lid of nails. *IEEE Microwave and Wireless Components Letters*, Vol. 20, No. 1:1–2, Jan 2010.
- [13] H.Merkel Z.Sipus and P.S Kildal. Green’s function for planar soft and hard surfaces derived by asymptotic boundary conditions. *IEEE Proc. Part H*, Vol. 47, No. 11:1–2, Oct. 1997.
- [14] A.Valero E.Alfonso, P.S Kildal and J.I.Hirranz. *IEEE AP-S*, Vol., July 2008.
- [15] David M.Pozar. *Microwave Engineering 3rd edition*. Wiley.
- [16] J.A Kempic D. Davis, O.J. Digiondomenic. A new type of circularly polarized antenna element. *Antennas and Propagation Society International Symposium*, Vol. 5:26–33, July 7 1967.
- [17] Helmut E. Schrank. Polarization measurements using the septum polarizer. *Antennas and Propagation Society International Symposium*, Vol. 20:227–230, Year 1982.
- [18] G.N. Tsandoulas Ming Hui Chen. A wideband square waveguide polarizer. *IEEE Transaction on Antennas and Propagation*, Vol.:1–2, May 1973.
- [19] P.-S. Kildal Eva. Rajo-Iglesias. Groove gap waveguide: A rectangular waveguide between contactless metal plates enabled by parallel-plate cut-off. *Antennas and propagation (EuCAP), 2010 proceedings*, Vol.:1–2, April 2010.

# MATLAB Code

---

```
function [AR, XPD]=AR(s31,s41,freq)
Septum Polarizer Performance Analysis

Eco=(s31+1i*s41)/sqrt(2);
Exp=(s31-1i*s41)/sqrt(2);
Eco_mag=abs(Eco);
Exp_mag=abs(Exp);
ratio=(Eco_mag+Exp_mag)./(Eco_mag-Exp_mag);
AR=20*log10(ratio);
b=freq;

Axial Ratio

fh = figure(1);
set(fh, 'color', 'white');
plot(freq,AR,'b','linewidth',2)
plot (freq(101:20:end),AR(101:20:end),'--r>','linewidth',1);
title('Axial Ratio');
xlabel('Frequency GHz','fontsize',18);
ylabel('Axial ratio dB','fontsize',18);
hold on
plot([40.5 40.5],[0 1.5],'k','linewidth',2);
hold on
plot([43.501 43.501],[0 1.5],'k','linewidth',2);
axis([39 45 0 0.5])
set(gca,'XTick', [39 40.5 41.5 42.5 43.5 45], 'YTick', [0:0.2:1.5]);
grid;

Cross Polar Isolation

ratio=abs(Exp./Eco);
XPD= 20*log10(ratio);
fh = figure(2);
set(fh, 'color', 'white');
plot(freq,XPD,'b','linewidth',2)
plot (freq(101:20:end),XPD(101:20:end),'--r>','linewidth',1);
title('Cross Polar Isolation');
xlabel('Frequency GHz','fontsize',18);
ylabel('Cross Polar Isolation dB','fontsize',18);
axis([40.5 43.5 10 50])
hold on
plot([40.5 40.5],[10 40],'k','linewidth',2);
hold on
plot([43.501 43.501],[10 40],'k','linewidth',2);
axis([39 45 0 0.5])
set(gca,'XTick', [39 40.5 41.5 42.5 43.5 45], 'YTick', [10:5:40]);
```

---

```

grid;
Relative Cross Polar Level

ratio=abs(Exp./Eco);
XP= 20*log10(ratio);
figure(3)
plot(freq,XP)
title('Relative Cross Polar Level');
xlabel('Frequency');
ylabel('Cross Polar Level dB');

```

---

```

%% Return Loss Performance %%

function return_loss(freq,SP)

s11=SP(:,1);
s22=SP(:,2);
s33=SP(:,3);
% s44=SP(:,4);

fh = figure(1);
set(fh, 'color', 'white');

plot (freq(1:20:end),s11(1:20:end),'--r*','linewidth',1);
hold on

plot (freq(1:20:end),s22(1:20:end),'--b*','linewidth',1);
hold on

plot (freq(1:20:end),s33(1:20:end),'--go','linewidth',1);
hold on

% plot (freq(1:5:end),s44(1:5:end),'--ms','linewidth',1);
% hold on

plot([40.5 40.5],[-50 -10],'k','linewidth',2);
hold on
plot([43.501 43.501],[-50 -10],'k','linewidth',2);

xlabel('Frequency GHz','fontsize',18);
ylabel('Isolation dB','fontsize',18);
legend('Proposed','CAD Based','Optimized');
set(gca,'XTick', [39 40.5 41.5 42.5 43.5 45], 'YTick', [-50:5:-10]);
grid;

```

---